Title: Bi-directional modification of sleep and wake by amyloid beta oligomers

One Sentence Summary: Amyloid beta acutely and size-dependently affects behavior through distinct wake- and sleep-promoting pathways.

Authors: Güliz Gürel Özcan[1], Sumi Lim[1], Patricia L.A. Leighton[2,3], W. Ted Allison[2,3], Jason Rihel[1*]

Affiliations:

1 Department of Cell and Developmental Biology, UCL, Gower Street, London, United Kingdom WC1E 6BT

2 Centre for Prions & Protein Folding Disease, University of Alberta, Edmonton AB, T6G 2M8, CANADA

3 Department of Biological Sciences, University of Alberta, Edmonton AB, T6G 2E9, CANADA

*correspondence: j.rihel@ucl.ac.uk

Abstract

Disrupted sleep is a major feature of Alzheimer's Disease (AD), often arising years before symptoms of cognitive decline. Prolonged wakefulness exacerbates the production of toxic amyloid-beta (Aβ) species, suggesting that sleep loss further accelerates AD progression. However, the mechanism by which Aβ affects sleep is unknown. We demonstrate here that Aβ acutely and reversibly enhances or suppresses sleep as a function of oligomer length. Genetic and pharmacological disruption revealed that short Aβ oligomers induce acute wakefulness

through Adrenergic receptor b2 (Adrb2) and Progesterone membrane receptor component 1 (Pgrmc1), while longer Aβ forms induce sleep through Prion Protein (PrP) signaling. We suggest that changes to the brain's balance of Aβ oligomeric species during AD progression disrupts the stability of a bi-directional, Aβ-sensitive sleep/wake switch.

Main Text

The first known event in Alzheimer's disease (AD) is an increase in soluble amyloid-beta (Aβ) with small changes in Aβ levels detectable years before the development of Aβ plaques and the onset of AD (*1-2*). Sleep disruption is also an early symptom of AD (*3*), and patients have sleep-wake abnormalities, including an increase in the amount of wakefulness at night and increased daytime napping (*4-6*). Multiple transgenic AD mouse models that overproduce Aβ also show disrupted sleep phenotypes (*7-9*), often in the absence of neuronal loss and preceding impairments of learning and memory (*10*). Understanding the relationship between Aβ accumulation, sleep disruption, and AD pathogenesis may therefore lead to better early detection and prevention of disease.

Some physiological changes, such as sleep, can alter the levels of extracellular Aβ (*11*). Aβ levels in the cerebrospinal fluid (CSF) increase during wake and decrease during sleep (*11, 12*), as the generation and release of both Aβ40 and Aβ42 are controlled by electrical and synaptic activity (*13, 14*). These observations have led to the proposal that sleep and Aβ dynamics create a vicious cycle, wherein increases in wakefulness result in increased extracellular Aβ and aggregation, which then dysregulates sleep, further exacerbating pathogenic Aβ production (*9*). How increased Aβ burden leads to disruptions in sleep remains unknown, although AD-related

cell death of critical sleep/wake regulatory neurons has been suggested as a possible mechanism (*15-17*).

We tested an alternative hypothesis that Aβ species directly signal to alter sleep/wake states. We took advantage of the ability to directly deliver small molecules and Aβ peptides to the brain of larval zebrafish, which unlike *Drosophila* have a conserved repertoire of amyloid precursor protein (APP) and its processing machinery. Moreover, sleep in zebrafish is diurnal and controlled by similar genetic, pharmacological, and neuronal mechanisms as mammals (*18*). We found that Aβ size-dependently and reversibly modulates behavior through two distinct genetic, pharmacologically tractable pathways that regulate sleep in opposing directions.

To test the acute signaling effects of Aβ on sleep, we developed a minimally invasive intra-cardiac injection assay in 5 days post fertilization (5dpf) larval zebrafish, which avoids direct damage to brain tissue (Fig. 1A). This technique rapidly (<1hr, peaking within 2-3hrs) and reversibly delivers Aβ to the larval brain, as assessed by injection of fluorescently tagged Aβ42 and subsequent confocal brain imaging (Fig. 1B and Fig. S1A-B). To generate different Aβ oligomeric species, we incubated Aβ42 overnight at increasing temperatures, which significantly varied the amount and lengths of Aβ oligomers as measured by Transmission Electron Microscopy (TEM) (Fig. 1C and S1C). Aβ42 incubated overnight at 4ºC consists of fewer and shorter oligomers ($A\beta^{short}$, mean 45±11 nm, median=39nm) than when incubated at 25ºC ($A\beta^{long}$, mean 75±10 nm, median=61nm) or at 37ºC ($A\beta^{v\text{-}long}$, mean 121±10 nm, median=88nm) (Fig. 1C).

We then assessed how each Aβ preparation affected sleep and wake behavior in zebrafish relative to an Aβ42-1 "reverse" peptide control ($A\beta^{rev}$) using video-monitoring (Fig. 1A) (*19,20*). In zebrafish larvae, sleep is defined as a period of inactivity lasting longer than one minute, as this is associated with an increased arousal threshold and other features of behavioral sleep (*19*). To determine the appropriate Aβ injection dose, we first injected 1nL of a 1-1000 nM dose response series for both $A\beta^{short}$ and $A\beta^{long}$ and found each species had opposing effects on larval sleep and waking activity (Fig. S1D-E), with maximal differences between these preparations at 10 nM ($p \leq 0.01$ doseXprep interaction, two-way ANOVA). As 1 nL of a 10 nM monomeric concentration of Aβ will yield a final estimated brain concentration <50 pM (see Methods), which is within the reported concentration ranges of Aβ42 in human CSF of 100 pM-5nM (*2*), we chose this dose for all subsequent experiments.

We found that Aβ42 affected sleep and wake in opposing directions depending on its oligomeric state (Fig. 1D-J). In the day following injection, $A\beta^{short}$ significantly increased waking activity (+19±6% relative to $A\beta^{rev}$) compared to $A\beta^{long}$ oligomers, which reduced waking activity by -9±5% (Fig. 1D-E, G). In contrast, $A\beta^{long}$ significantly increased sleep during the post-injection day by +19±8% while $A\beta^{short}$ decreased total sleep by -12±9% (Fig. 1D'-E', I). Increased sleep induced by $A\beta^{long}$ was due to a significant increase in the average sleep bout length (Fig. 1I) but also due to a modest increase in the number of sleep bouts (Fig. 1J), indicating higher sleep initiation and consolidation. Injection of longer Aβ fibers ($A\beta^{v\_long}$) had neither the wake-promoting effect of $A\beta^{short}$ nor the sleep-promoting effect of $A\beta^{long}$ (Fig. 1F-J), demonstrating that Aβ's biological activity *in vivo* is narrowly size-dependent. There were no significant differences in sleep or waking activity among the Aβ preparations the night following injection (Fig. S1J-K).

Several lines of evidence suggest the dual-effects of Aβ on sleep and wake are due to acute signalling and not to long-term toxic effects from neuronal damage or death. First, injected animals returned to baseline sleep and activity levels within 24 hours (Fig. S1F-I). Second, injection with Aβ42 had no effect on apoptosis, as detected by staining for activation of Caspase-3 (Fig. S2A-C). Finally, Aβ injected animals raised to adulthood showed no major differences in their general health or in their survival rates (Fig. S2D). We therefore sought to identify the neuronal and molecule substrates through which Aβ signals to modulate sleep/wake behavior.

If Aβ oligomers alter behavior through acute signalling in the brain, the differential effects of $A\beta^{short}$ and $A\beta^{long}$ should be reflected at the level of neuronal activity. In situ hybridization (ISH) for expression of the immediate early gene, *c-fos*, identified several areas of the larval brain that are upregulated after injection of $A\beta^{short}$ relative to $A\beta^{rev}$, including the posterior hypothalamus and the dorsal and ventral telencephalon (Fig. 2A), which are also upregulated in hyperactive zebrafish mutants[21]. In contrast, *c-fos* expression following $A\beta^{long}$ injections was globally dampened relative to $A\beta^{rev}$ (Fig. 2B). Because immediate early gene expression is an imperfect readout of changes in neuronal activity, we also used the MAP-Mapping technique to visualize the relative brain-wide changes in phosphorylated ERK levels, which strongly correlates with neuronal activity levels in zebrafish larvae (*22*). Consistent with *c-fos*, $A\beta^{short}$ upregulated P-ERK in the ventral telencephalon and posterior hypothalamus (Fig. 2C, C' and Supplementary Data 1), while $A\beta^{long}$ resulted in a widespread reduction in P-ERK levels throughout most of the brain (Fig. 2D, D' and Supplementary Data 2). These neuronal activity maps are consistent with the sleep and wake behavioral changes induced by $A\beta^{short}$ and $A\beta^{long}$.

Many putative Aβ binding partners have been implicated in mediating the toxic signalling effects of Aβ on synapses, with some targets showing preferences for Aβ dimers, such as adrenergic receptor β2 (Adrb2) (*23*), or low molecular weight (50-75 kDa) species, such as the progesterone membrane receptor component 1 (PGRMC1) (*24*), while other targets preferentially bind to longer oligomers/protofibrils, such as the Prion Protein (PrP) (*25,26*). We therefore made genetic lesions in candidate Aβ receptors (Fig S3, S5) and tested whether these had any effect on $A\beta^{short}$-induced waking activity. Although *adrb2a*$^{-/-}$ and *pgrmc1*$^{-/-}$ exhibited only minor changes in baseline sleep and wake on a 14hr:10hr light:dark cycle (Fig S4A-F'), they had profoundly altered responses after injection of $A\beta^{short}$: Neither mutant increased waking activity (Fig. 3A-C,E) or suppressed sleep as observed in wild type controls (Fig. 3A'-C',F). Injection of $A\beta^{short}$ into *adrb2a*$^{-/-}$ animals even significantly increased sleep instead of reducing it as in wild type larvae (Fig. 3B',F). In contrast, $A\beta^{short}$ injected into mutants that lack both zebrafish Prp orthologs (*prp1*$^{-/-}$*; prp2*$^{-/-}$) (*27,28*) elicited even stronger increases in waking activity and reductions in sleep (Fig. 3D-F). Thus, the wake-promoting activity of $A\beta^{short}$ requires intact Adrb2a and Pgrmc1 but not functional Prp1 and Prp2.

Because the oligomeric species in the $A\beta^{long}$ preparation falls into the range that interacts with Prion Protein (PrP) with high affinity to modulate synapses (*25,26,29,30*), we tested whether PrP is instead required for $A\beta^{long}$-induced sleep. Under baseline conditions, we detected no significant differences in day or night sleep and waking activity in *prp* mutants compared to *prp*$^{+/+}$ siblings generated from either *prp1*$^{+/-}$*; prp2*$^{+/-}$ or *prp1*$^{+/-}$*;prp2*$^{-/-}$ in-crosses (Fig S6A-F'). However, after injection of $A\beta^{long}$, *prp1*$^{-/-}$*;prp2*$^{-/-}$ null mutants failed to increase sleep (-12±8% vs. +64±17% change in wild type sleep, Fig. 4A-D). Zebrafish have a third PrP ortholog (Prp3) with conserved GPI and repetitive prion protein domains but lacking all recognizable Aβ binding

regions (Fig. S5A,B). To ensure all Prp function was eliminated, we made genetic lesions in *prp3* (Fig. S5C,D) and found that the blockade of $A\beta^{long}$–induced sleep in *prp1*$^{-/-}$;*prp2*$^{-/-}$ double mutants was not additionally modulated by *prp3*$^{-/-}$ (Fig. S7B,D). Thus, while Prps are not required for the wake-inducing effects of $A\beta^{short}$, functional Prp1 and Prp2 are essential for sleep induced by $A\beta^{long}$.

If $A\beta^{long}$ interacts directly with Prp to drive changes in sleep, pharmacological manipulations known to disrupt this signalling cascade should similarly block the sleep-promoting effect of $A\beta^{long}$ (Fig. 4E). Consistent with a role for direct $A\beta^{long}$-Prp interactions in sleep, soaking the larvae in Chicago Sky Blue 6B, a small molecule reported to disrupt Aβ-PrP interactions (*31*), significantly abolished the sleep-inducing effect of $A\beta^{long}$ (Fig. 4F-G, S7E-F). Similarly, pharmacological inhibition of the putative Aβ-Prp downstream signalling components mGluR5 and Fyn kinase (*30,32*) significantly blocked the sleep-inducing properties of $A\beta^{long}$ (Fig. 4H-K, S7G-H). Both the mGluR5 inhibitor MPEP and the Src-kinase inhibitor saracatinib even resulted in significant sleep reductions after exposure to $A\beta^{long}$, consistent with $A\beta^{long}$-Prp activating this pathway to signal sleep and oppose the wake-promoting effects of $A\beta^{short}$. Thus, both genetic and pharmacological interference with Aβ-Prp signalling prevents the ability of $A\beta^{long}$ to increase sleep behavior.

Previous studies have suggested that changes in sleep during AD may further accelerate Aβ accumulation and neuronal damage, creating a viscous cycle that leads to further neuronal dysregulation and increased sleep-wake cycle abnormalities (*9*). Our results show that Aβ42 can acutely change sleep and wake depending on its oligomeric form, independently of neuronal

death. Not only does our data identify behaviorally relevant targets of Aβ, but our proposed bi-directional model for Aβ sleep/wake regulation (Fig. 4L) predicts that alterations to the relative concentrations of Aβ oligomers during healthy aging and AD disease progression will have dual consequences on sleep and wake states.

Many potential receptors of Aβ have been proposed, but controversy surrounds both the nature of the oligomeric species that interacts with each target and their relative importance during progressive cognitive decline and other phenotypes associated with AD (*33*). We identified a wake-promoting pathway requiring Adrb2a and Pgrmc1 that is activated by shorter Aβ species and a distinct, Prp-dependent sleep-promoting pathway activated by longer oligomers. Since AD brain extracts have been shown to activate both PGRMC1 (*24*) and Prp-signalling (*34*), both signalling pathways may be directly relevant in AD sleep/wake regulation. However, our identification of Aβ targets that are activated *in vivo* at low concentrations to alter behavior also reveals potential roles for Aβ signalling in non-diseased contexts.

The Aβ assembly process is highly complex and meta-stability is an intrinsic property of Aβ solutions[35]. While the precise makeup of Aβ species present in healthy and AD brains remains difficult to determine, several studies have demonstrated that the amount and type of Aβ oligomeric species (including dimer, trimers, and 56 kDa oligomers) in healthy brains change across the human life cycle (*36*) and are heterogeneous and elevated in AD patients (*34*,*37*). Our data suggests that changes in the relative concentration of sleep- and wake- promoting Aβ oligomeric species over the course of both healthy aging and AD will signal either increases or decreases in sleep (Fig. 4L). On shorter time-scales, sleep deprivation acutely increases Aβ

burden (*38*), fever promotes amyloidogenic Aβ generation (*39*), and microbial infection can trigger Aβ fibrilization (*40*). Considering that infection and fever are also potent drivers of sleep (*41*), the Aβ-Prp sleep signalling module identified here could mediate recovery sleep during illness and should be the subject of future studies. On longer timescales, AD progression is associated with increasingly large disruptions in sleep patterns, with patients exhibiting high levels of sleep fragmentation, a lack of circadian rhythm, night-time insomnia and irregular daytime napping throughout the day (*42*). Based on our results, the sleep symptoms associated with normal aging and AD may reflect changes in Aβ burden that lead to altered sleep signalling via molecular cascades that are potential therapeutic targets for treating disrupted sleep early in AD progression.

References and Notes:

1. Jack, C. R. *et al.* Tracking pathophysiological processes in Alzheimer's disease: an updated hypothetical model of dynamic biomarkers. *Lancet Neurol.* **12**, 207–216 (2013).
2. Bateman, R. J., Wen, G., Morris, J. C. & Holtzman, D. M. Fluctuations of CSF amyloid-beta levels: implications for a diagnostic and therapeutic biomarker. *Neurology* **68**, 666–669 (2007).
3. Sterniczuk, R., Theou, O., Rusak, B. & Rockwood, K. Sleep disturbance is associated with incident dementia and mortality. *Curr. Alzheimer Res.* **10**, 767–775 (2013).
4. Allen, S. R., Seiler, W. O., Stähelin, H. B. & Spiegel, R. Seventy-two hour polygraphic and behavioral recordings of wakefulness and sleep in a hospital geriatric unit: comparison between demented and nondemented patients. *Sleep* **10**, 143–159 (1987).

5. Loewenstein, R. J. *et al.* Disturbances of sleep and cognitive functioning in patients with dementia. *Neurobiol. Aging* **3**, 371–377 (1982).
6. Prinz, P. N. *et al.* Sleep, EEG and mental function changes in senile dementia of the Alzheimer's type. *Neurobiol. Aging* **3**, 361–370 (1982).
7. Wang, J., Ikonen, S., Gurevicius, K., van Groen, T. & Tanila, H. Alteration of cortical EEG in mice carrying mutated human APP transgene. *Brain Res.* **943**, 181–190 (2002).
8. Sterniczuk, R., Dyck, R. H., Laferla, F. M. & Antle, M. C. Characterization of the 3xTg-AD mouse model of Alzheimer's disease: part 1. Circadian changes. *Brain Res.* **1348**, 139–148 (2010).
9. Roh, J. H. *et al.* Disruption of the sleep-wake cycle and diurnal fluctuation of β-amyloid in mice with Alzheimer's disease pathology. *Sci. Transl. Med.* **4**, 150ra122 (2012).
10. Irizarry, M. C., McNamara, M., Fedorchak, K., Hsiao, K. & Hyman, B. T. APPSw transgenic mice develop age-related A beta deposits and neuropil abnormalities, but no neuronal loss in CA1. *J. Neuropathol. Exp. Neurol.* **56**, 965–973 (1997).
11. Kang, J.-E. *et al.* Amyloid-beta dynamics are regulated by orexin and the sleep-wake cycle. *Science* **326**, 1005–1007 (2009).
12. Xie, L. *et al.* Sleep drives metabolite clearance from the adult brain. *Science* **342**, 373–377 (2013).
13. Cirrito, J. R. *et al.* Synaptic activity regulates interstitial fluid amyloid-beta levels in vivo. *Neuron* **48**, 913–922 (2005).
14. Kamenetz, F. *et al.* APP processing and synaptic function. *Neuron* **37**, 925–937 (2003).

15. Lim, A. S. P. *et al.* Sleep is related to neuron numbers in the ventrolateral preoptic/intermediate nucleus in older adults with and without Alzheimer's disease. *Brain J. Neurol.* **137**, 2847–2861 (2014).
16. Fronczek, R. *et al.* Hypocretin (orexin) loss in Alzheimer's disease. *Neurobiol. Aging* **33**, 1642–1650 (2012).
17. Manaye, K. F. *et al.* Age-related loss of noradrenergic neurons in the brains of triple transgenic mice. *Age Dordr. Neth.* **35**, 139–147 (2013).
18. Barlow, I. L. & Rihel, J. Zebrafish sleep: from geneZZZ to neuronZZZ. *Curr. Opin. Neurobiol.* **44**, 65–71 (2017).
19. Prober, D. A., Rihel, J., Onah, A. A., Sung, R.-J. & Schier, A. F. Hypocretin/orexin overexpression induces an insomnia-like phenotype in zebrafish. *J. Neurosci. Off. J. Soc. Neurosci.* **26**, 13400–13410 (2006).
20. Rihel, J. *et al.* Zebrafish behavioral profiling links drugs to biological targets and rest/wake regulation. *Science* **327**, 348–351 (2010).
21. Ashlin, T. G., Blunsom, N. J., Ghosh, M., Cockcroft, S. & Rihel, J. Pitpnc1a Regulates Zebrafish Sleep and Wake Behavior through Modulation of Insulin-like Growth Factor Signaling. *Cell Rep.* **24**, 1389–1396 (2018).
22. Randlett, O. *et al.* Whole-brain activity mapping onto a zebrafish brain atlas. *Nat. Methods* **12**, 1039–1046 (2015).
23. Wang, D. *et al.* Binding of amyloid beta peptide to beta2 adrenergic receptor induces PKA-dependent AMPA receptor hyperactivity. *FASEB J. Off. Publ. Fed. Am. Soc. Exp. Biol.* **24**, 3511–3521 (2010).

24. Izzo, N. J. *et al.* Alzheimer's therapeutics targeting amyloid beta 1-42 oligomers II: Sigma-2/PGRMC1 receptors mediate Abeta 42 oligomer binding and synaptotoxicity. *PloS One* **9**, e111899 (2014).
25. Laurén, J., Gimbel, D. A., Nygaard, H. B., Gilbert, J. W. & Strittmatter, S. M. Cellular prion protein mediates impairment of synaptic plasticity by amyloid-beta oligomers. *Nature* **457**, 1128–1132 (2009).
26. Nicoll, A. J. *et al.* Amyloid-β nanotubes are associated with prion protein-dependent synaptotoxicity. *Nat. Commun.* **4**, 2416 (2013).
27. Fleisch, V. C. *et al.* Targeted mutation of the gene encoding prion protein in zebrafish reveals a conserved role in neuron excitability. *Neurobiol. Dis.* **55**, 11–25 (2013).
28. Leighton, P. L. A., Kanyo, R., Neil, G. J., Pollock, N. M. & Allison, W. T. Prion gene paralogs are dispensable for early zebrafish development and have nonadditive roles in seizure susceptibility. *J. Biol. Chem.* **293**, 12576–12592 (2018).
29. Gimbel, D. A. *et al.* Memory impairment in transgenic Alzheimer mice requires cellular prion protein. *J. Neurosci. Off. J. Soc. Neurosci.* **30**, 6367–6374 (2010).
30. Um, J. W. *et al.* Alzheimer amyloid-β oligomer bound to postsynaptic prion protein activates Fyn to impair neurons. *Nat. Neurosci.* **15**, 1227–1235 (2012).
31. Risse, E. *et al.* Identification of a Compound That Disrupts Binding of Amyloid-β to the Prion Protein Using a Novel Fluorescence-based Assay. *J. Biol. Chem.* **290**, 17020–17028 (2015).
32. Um, J. W. *et al.* Metabotropic glutamate receptor 5 is a coreceptor for Alzheimer aβ oligomer bound to cellular prion protein. *Neuron* **79**, 887–902 (2013).

33. Benilova, I., Karran, E. & De Strooper, B. The toxic Aβ oligomer and Alzheimer's disease: an emperor in need of clothes. *Nat. Neurosci.* **15**, 349–357 (2012).

34. Kostylev, M. A. *et al.* Prion-Protein-interacting Amyloid-β Oligomers of High Molecular Weight Are Tightly Correlated with Memory Impairment in Multiple Alzheimer Mouse Models. *J. Biol. Chem.* **290**, 17415–17438 (2015).

35. Teplow, D. B. Preparation of amyloid beta-protein for structural and functional studies. *Methods Enzymol.* **413**, 20–33 (2006).

36. Lesné, S. E. *et al.* Brain amyloid-β oligomers in ageing and Alzheimer's disease. *Brain J. Neurol.* **136**, 1383–1398 (2013).

37. Izzo, N. J. *et al.* Alzheimer's therapeutics targeting amyloid beta 1-42 oligomers I: Abeta 42 oligomer binding to specific neuronal receptors is displaced by drug candidates that improve cognitive deficits. *PloS One* **9**, e111898 (2014).

38. Shokri-Kojori, E. *et al.* β-Amyloid accumulation in the human brain after one night of sleep deprivation. *Proc. Natl. Acad. Sci. U. S. A.* **115**, 4483–4488 (2018).

39. Szaruga, M. *et al.* Alzheimer's-Causing Mutations Shift Aβ Length by Destabilizing γ-Secretase-Aβn Interactions. *Cell* **170**, 443–456.e14 (2017).

40. Eimer, W. A. *et al.* Alzheimer's Disease-Associated β-Amyloid Is Rapidly Seeded by Herpesviridae to Protect against Brain Infection. *Neuron* **99**, 56–63.e3 (2018).

41. Imeri, L. & Opp, M. R. How (and why) the immune system makes us sleep. *Nat. Rev. Neurosci.* **10**, 199–210 (2009).

42. Videnovic, A., Lazar, A. S., Barker, R. A. & Overeem, S. 'The clocks that time us'--circadian rhythms in neurodegenerative disorders. *Nat. Rev. Neurol.* **10**, 683–693 (2014).

43. Guo, Y., Veneman, W. J., Spaink, H. P. & Verbeek, F. J. Three-dimensional reconstruction and measurements of zebrafish larvae from high-throughput axial-view in vivo imaging. *Biomed. Opt. Express* **8**, 2611–2634 (2017).

44. Gagnon, J. A. *et al.* Efficient mutagenesis by Cas9 protein-mediated oligonucleotide insertion and large-scale assessment of single-guide RNAs. *PloS One* **9**, e98186 (2014).

45. Cotto, E., André, M., Forgue, J., Fleury, H. J. & Babin, P. J. Molecular characterization, phylogenetic relationships, and developmental expression patterns of prion genes in zebrafish (Danio rerio). *FEBS J.* **272**, 500–513 (2005).

Acknowledgements:

We thank Dr. Tom Hawkins and Mark Turmaine for assistance with TEM, Dr. Gaia Gestri for assistance with heart injections and Dr. Marcus Ghosh for assistance with tERK/pERK experiments. We also thank Dr. Dervis Salih, Prof. Steve Wilson and Prof. John Hardy for their comments and all first-floor fish lab members for their input throughout the project. **Funding:** This was supported by operating funds to WTA from the Alzheimer Society of Alberta & Northwest Territories and Alberta Prion Research Institute of Alberta Innovates. PLAL was supported by Alzheimer Society of Canada, and JR was funded by an Interdisciplinary Research Grant from the Alzheimer's Research UK, an ERC starting grant, and a UCL Excellence Fellowship. **Author Contributions:** GGO and JR conceived and designed the experiments. GGO performed all experiments with assistance from SL. GGO, JR, and SL analysed the data. GGO and SL generated the *prp3*, *adrb2a* and *pgrmc1* mutants. PLAL and WTA generated the *prp1* and *prp2* mutants. GGO and JR wrote the manuscript with input from all authors. **Competing interests:** The authors declare no competing interests. **Data and materials**

availability: All data is available in the manuscript or the supplementary materials.

List of Supplementary Materials:

Materials and Methods

Fig S1-S7

Supplemental Data 1-2

<u>Figure 1</u>. Aβ oligomers bi-directionally affect sleep and wake in zebrafish larvae.

A) Aβ was injected into the heart of 5 dpf larvae in the morning (ZT2= zeitgeber time 2, i.e. 2hr after lights on) and behavior was transferred to a 96-well plate and monitored for 24 hours on a 14:10 light:dark cycle.

B) Heart-injected HiLyte™ Fluor 647-labeled Aβ (fAβ) penetrated the whole larval brain as visualized by confocal microscopy (optical sections, dorsal view) taken 2 hr after injection. Anterior is to the top.

C) Aβ prepared under increasing temperatures adopted longer oligomeric lengths, as measured by electron microscopy. **$p \leq 0.01$, ****$p \leq 1x10^{-7}$ Kruskal-Wallis, Tukey-Kramer post-hoc test. The bars show the median. Data was taken from five randomly selected micrographs from two independent experiments.

D-F') Exemplar 24-hr traces post-injection comparing the effect of Aβ preparations on average waking activity (D-F) and sleep (D'-F') versus Aβ reverse peptide controls. Ribbons represent ± the standard error of the mean (SEM). Light and dark bars indicate the lights ON and lights OFF periods, respectively.

G-J) Each graph plots the percent change in post-injection daytime activity (G), sleep (H), sleep bout length (I), and sleep bout number (J) relative to Aβ reverse injections. *$p \leq 0.05$, **$p \leq 0.01$, $^{ns}p > 0.05$, Kruskal-Wallis, Tukey-Kramer post-hoc. Each dot represents a single larva and error bars indicate ± SEM. Data is pooled from 4 independent experiments for each Aβ type.

<u>Figure 2</u>. Aβ oligomers differentially alter neuronal activity in the larval zebrafish brain.

A) As detected by ISH, the immediate early gene *c-fos* is upregulated in many larval brain areas following $A\beta^{short}$ injection, including the dorsal and ventral telencephalon (Tel) and the posterior hypothalamus (black arrowheads), relative to Aβ reverse control injections. Hyp- Hypothalamus; Hb- Hindbrain.

B) Compared to $A\beta^{rev}$ injections, $A\beta^{long}$ oligomers induce less *c-fos* expression. The $A\beta^{rev}$ and $A\beta^{long}$ treated brains were stained longer than in panel A) to ensure capture of even weak *c-fos* expression.

C-C') Brain expression of the neuronal activity correlate pERK/tERK comparing $A\beta^{short}$ (n =6) to $A\beta^{rev}$ (n = 5) injected larvae identifies areas upregulated (green) and downregulated (magenta) by $A\beta^{short}$. Data are shown as a thresholded maximum projection overlaid on the Z-Brain tERK reference (gray). White arrowheads indicate regions in the ventral telencephalon and posterior hypothalamus that are upregulated similar to *c-fos* in A). Dorsal view in C), lateral view in C').

D-D') pERK/tERK expression after $A\beta^{long}$ injections (n=7) shows widespread downregulation of neuronal activity (magenta) compared to $A\beta^{rev}$ controls (n=7), consistent with *c-fos* data in B. Dorsal view in D), lateral view in D').

<u>Figure 3</u>. Wake induction by $A\beta^{short}$ requires Adrb2a and Pgrmc1, but not the Prion Protein.

A-D') Exemplar 24-hr traces comparing the effects of $A\beta^{short}$ oligomers on average waking activity (A-D) and sleep (A'-D') versus $A\beta^{rev}$ on wild type (A,A'), *adrb2a*$^{-/-}$ (B,B'), *pgrmc1*$^{-/-}$ (C,C'), and *prp1*$^{-/-}$;*prp2*$^{-/-}$ mutant (D,D') backgrounds. Ribbons represent ± the standard error of the mean (SEM). Light and dark bars indicate the lights ON and lights OFF periods, respectively.

E-F) Graphs plot the percent change in waking activity (E) and sleep (F) induced by $A\beta^{short}$ relative to reverse Aβ control injections on wild type and mutant backgrounds, with dotted line at zero indicating $A\beta^{short}$ oligomers had zero detectable effect. The wake enhancing and sleep suppressing effects of $A\beta^{short}$ is absent in *adrb2a*$^{-/-}$ and *pgrmc1*$^{-/-}$, but present in *prp1*$^{-/-}$;*prp2*$^{-/-}$ mutants, wherein the effects of $A\beta^{short}$ are enhanced. $^{ns}p>0.05$, $*p\leq0.05$, $**p\leq0.01$, $***p\leq0.0001$, $****p\leq10^{-5}$ Kruskal-Wallis, Bonferroni corrected. Each dot represents a single larva and error bars indicate ± SEM. Data is pooled from n=2 independent experiments for *adrb2a*$^{-/-}$ and *pgrmc1*$^{-/-}$ and n=3 for *prp1*$^{-/-}$;*prp2*$^{-/-}$.

<u>Figure 4</u>. Sleep induction by $A\beta^{long}$ requires signalling through Prion Protein

A-B') Exemplar 24-hr traces comparing the effects of $A\beta^{long}$ oligomers on average waking activity (A,B) and sleep (A'-B') versus $A\beta^{rev}$ on wild type (A,A'), and *prp1*$^{-/-}$;*prp2*$^{-/-}$ mutant (B,B') backgrounds. Ribbons represent ± the standard error of the mean (SEM). Light and dark bars indicate the lights ON and lights OFF periods, respectively.

C-D) Graphs plot the percent change in waking activity (C) and sleep (D) induced by $A\beta^{long}$ relative to Aβ reverse control injections on wild type and *prp1*$^{-/-}$;*prp2*$^{-/-}$ mutant backgrounds (mixed *prp3* background). The sleep promoting effect of $A\beta^{long}$ is blocked in *prp1*$^{-/-}$;*prp2*$^{-/-}$ mutants. $**p\leq0.01$, Kruskal-Wallis. Each dot represents a single larva and error bars indicate ± SEM.

E) Schematic showing how Aβ – Prp interactions are thought to signal through activation of Fyn kinase. Small molecules that block each step in the pathway are indicated.

F) Representative traces of sleep behavior after $A\beta^{long}$ versus $A\beta^{rev}$ injections in the absence (top) or presence (bottom) of the Aβ-Prion disruptor, Chicago Sky Blue (3nM). Ribbons represent ± SEM. Light and dark bars indicate the lights ON and lights OFF periods, respectively.

G) The percent change in sleep induced by $A\beta^{long}$ relative to $A\beta^{rev}$ control injections in the absence or presence of 3nM Chicago Sky Blue. **$p \leq 0.01$, Kruskal-Wallis. Each dot represents a single larva from n= 2 independent experiments and error bars indicate ± SEM.

H-J) Representative traces of sleep behavior after $A\beta^{long}$ versus $A\beta^{rev}$ injections in the absence (H) or presence of the Src-kinase inhibitor, saracatinib at 300 nM (I) or mGluR5 inhibitor, MPEP (5 µM) (J). Ribbons represent ± SEM.

K) The percent change in sleep relative to reverse Aβ control injections in the absence or presence of MPEP (5µM) and 300 nM saracatinib. **$p \leq 0.01$, ***$p \leq 1x10^{-6}$ Kruskal-Wallis, Bonferroni. Each dot represents a single larva and error bars indicate ± SEM. Data is pooled from 2 independent experiments.

L) A bi-directional model for sleep/wake regulation by Aβ. In wild type animals (centre), injection of $A\beta^{short}$ and $A\beta^{long}$ signal through Adrb2a and PrP to suppress or drive sleep, respectively. Because Aβ preparations are a mixture of long and short forms, the behavioral output is the summation of both signalling arms. In mutants that lack PrP (left), only the short, wake-promoting Aβ species contribute to behavioral responses, while in mutants that lack Adrb2a/Pgrmc1 (right), only the long, sleep-promoting Aβ species affect behavior.

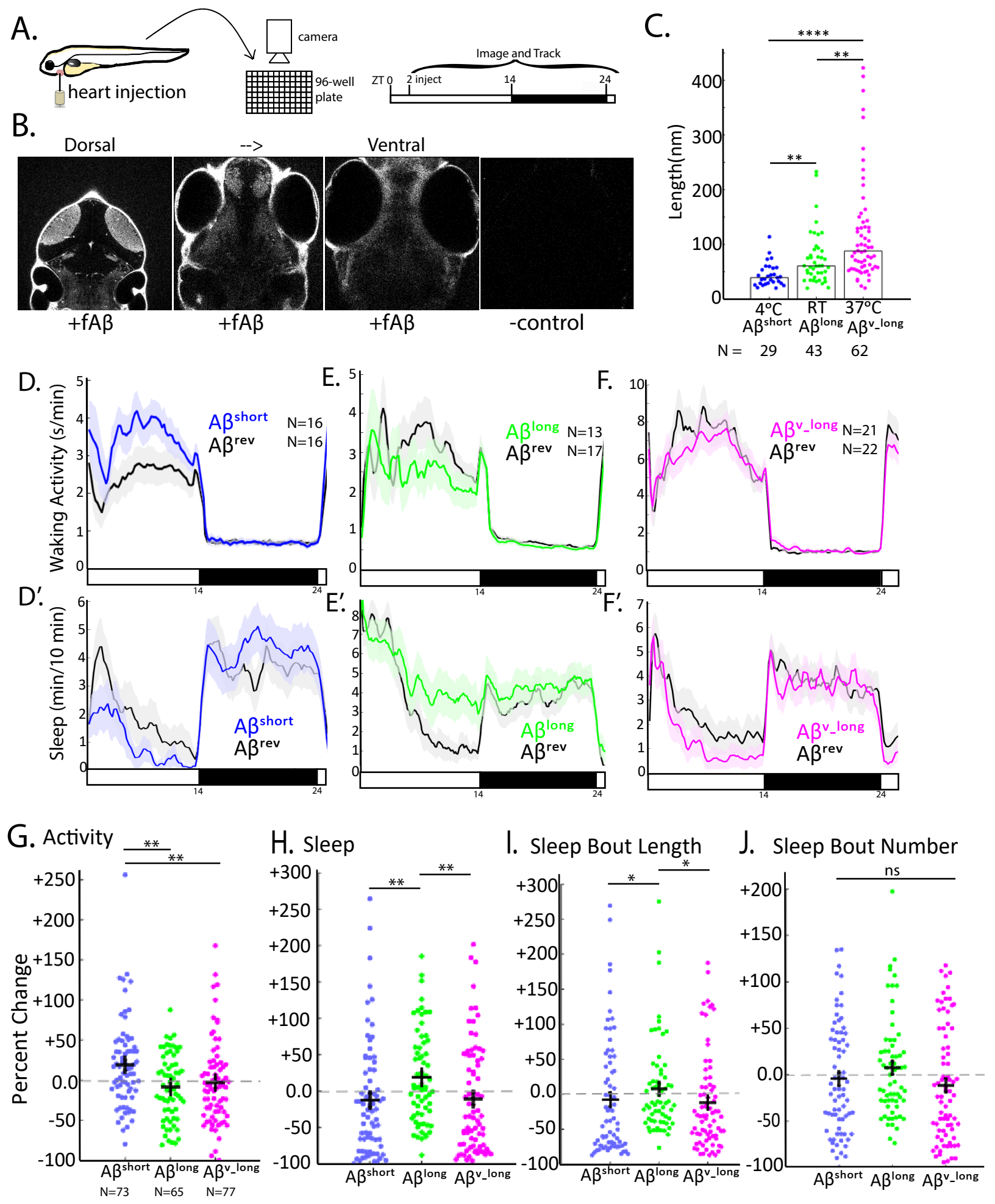
A.
heart injection
camera
96-well plate
Image and Track
ZT 0
2 inject
14
24
B.
Dorsal
-->
Ventral
+fAβ
+fAβ
+fAβ
-control
C.
Length(nm)
4°C
RT
37°C
Aβshort
Aβlong
Aβv_long
N = 29 43 62
D.
Waking Activity (s/min)
Aβshort N=16
Aβrev N=16
E.
Aβlong N=13
Aβrev N=17
F.
Aβv_long N=21
Aβrev N=22
D'.
Sleep (min/10 min)
E'.
F'.
G. Activity
Percent Change
Aβshort N=73
Aβlong N=65
Aβv_long N=77
H. Sleep
I. Sleep Bout Length
J. Sleep Bout Number
ns

Figure 1

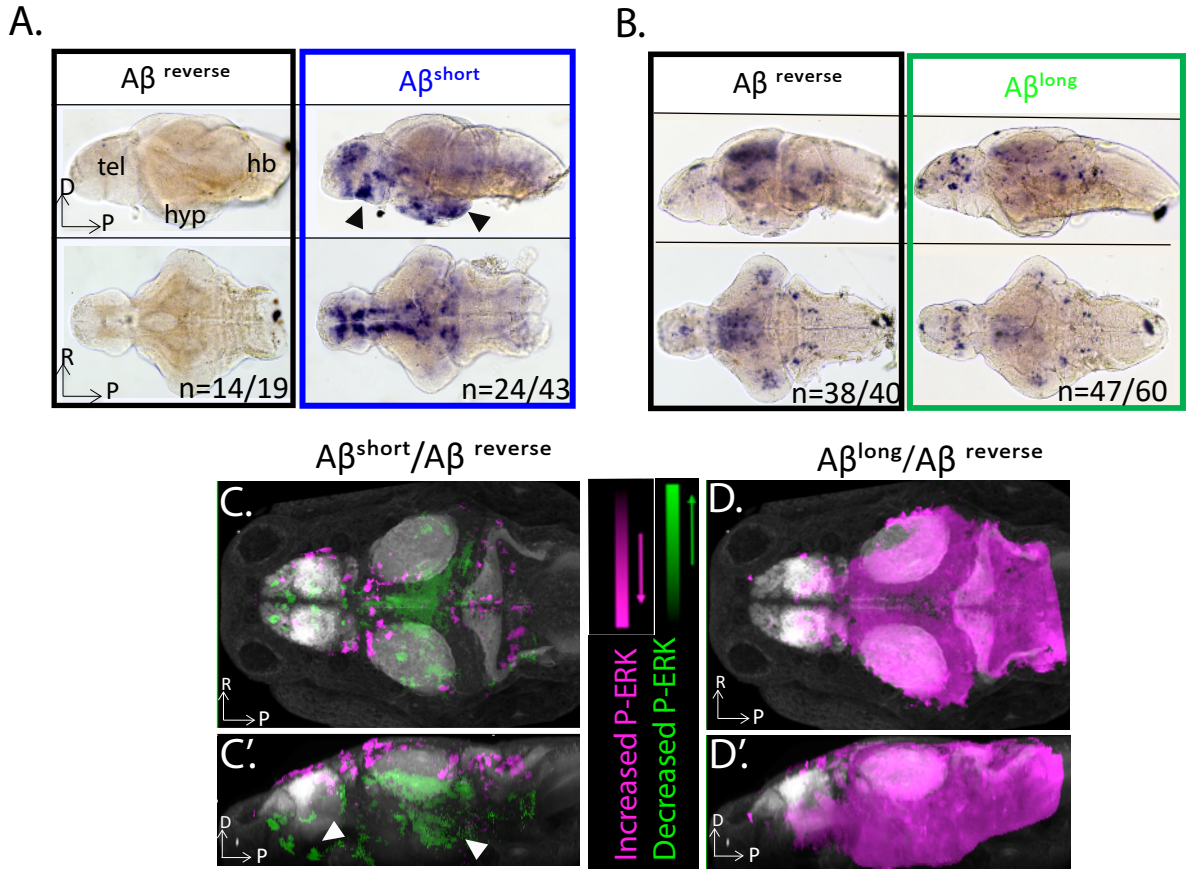
A.
Aβ reverse
Aβshort
tel
hb
hyp
D
P
R
P
n=14/19
n=24/43
B.
Aβ reverse
Aβlong
n=38/40
n=47/60
Aβshort/Aβ reverse
Aβlong/Aβ reverse
C.
C′.
D.
D′.
Increased P-ERK
Decreased P-ERK

Figure 2

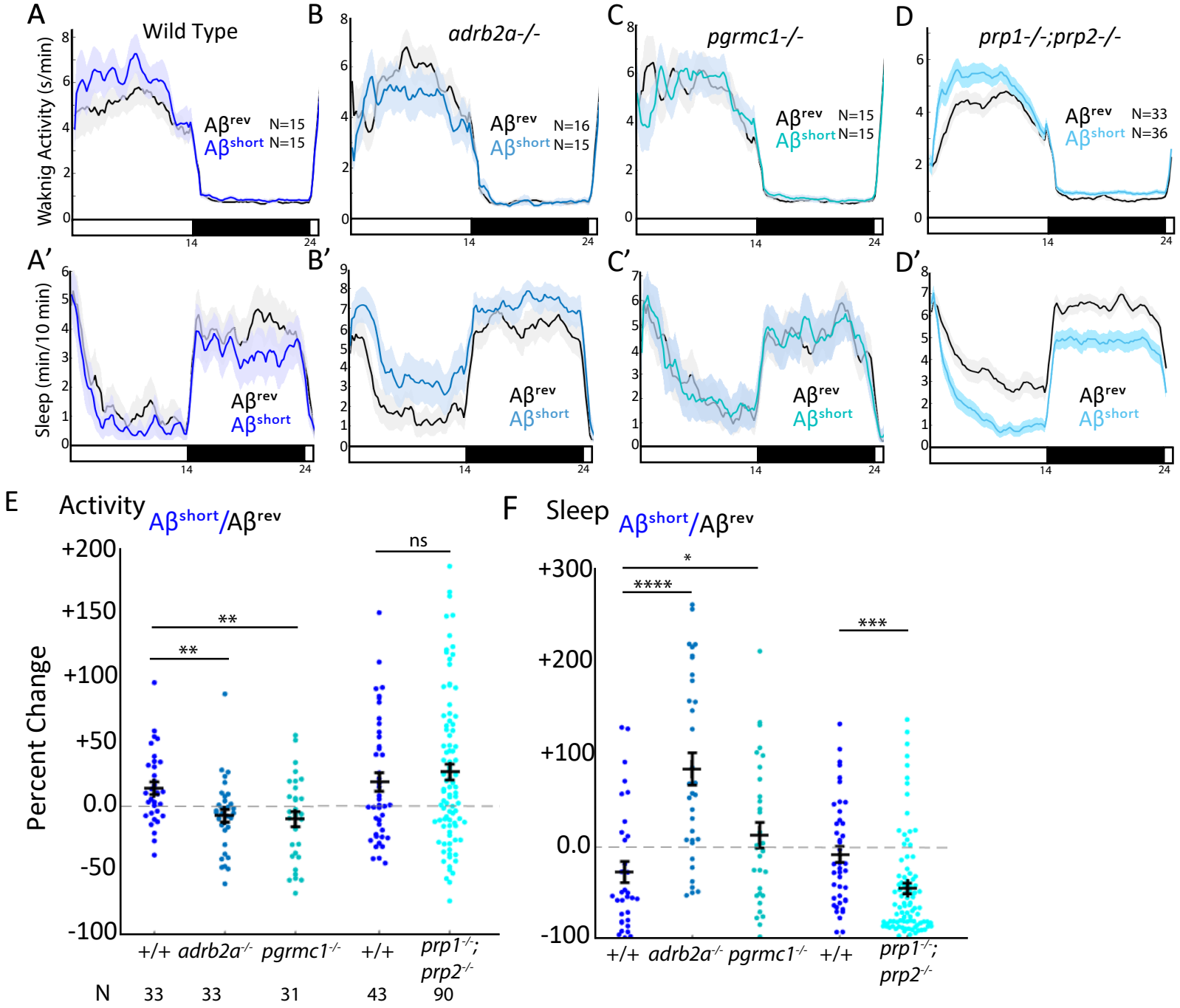
A
Wild Type
Waknig Activity (s/min)
Aβrev N=15
Aβshort N=15
B
adrb2a-/-
Aβrev N=16
Aβshort N=15
C
pgrmc1-/-
Aβrev N=15
Aβshort N=15
D
prp1-/-;prp2-/-
Aβrev N=33
Aβshort N=36
A'
Sleep (min/10 min)
B'
C'
D'
E
Activity
Aβshort/Aβrev
Percent Change
ns
**
**
+/+
adrb2a-/-
pgrmc1-/-
+/+
prp1-/-; prp2-/-
N 33 33 31 43 90
F
Sleep
Aβshort/Aβrev
*
****
***

Figure 3

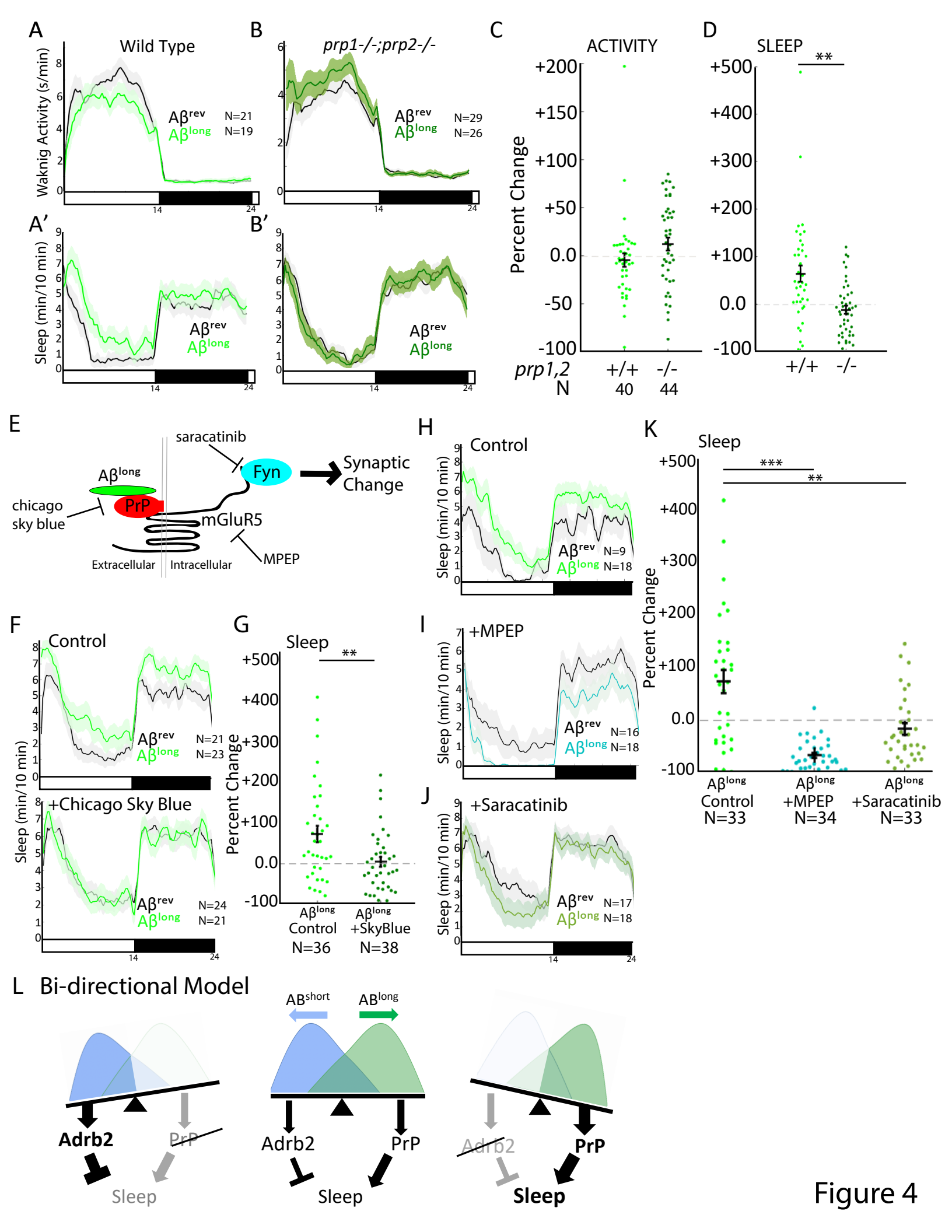
A
Wild Type
Waknig Activity (s/min)
Aβrev N=21
Aβlong N=19
B
prp1-/-;prp2-/-
Aβrev N=29
Aβlong N=26
A'
Sleep (min/10 min)
B'
C
ACTIVITY
Percent Change
prp1,2 +/+ -/-
N 40 44
D
SLEEP
**
+/+ -/-
E
saracatinib
Fyn
Synaptic Change
Aβlong
PrP
chicago sky blue
mGluR5
MPEP
Extracellular
Intracellular
F
Control
Aβrev N=21
Aβlong N=23
+Chicago Sky Blue
Aβrev N=24
Aβlong N=21
G
Sleep
**
Aβlong Control N=36
Aβlong +SkyBlue N=38
H
Control
Aβrev N=9
Aβlong N=18
I
+MPEP
Aβrev N=16
Aβlong N=18
J
+Saracatinib
Aβrev N=17
Aβlong N=18
K
Sleep
***
**
Aβlong Control N=33
Aβlong +MPEP N=34
Aβlong +Saracatinib N=33
L Bi-directional Model
ABshort
ABlong
Adrb2
PrP
Sleep
Adrb2
PrP
Sleep
Adrb2
PrP
Sleep

Figure 4

Supplementary Materials (Ozcan et al.)

Materials and Methods:

Zebrafish strains and husbandry

Zebrafish (Danio rerio) were raised under standard conditions at 28°C in a 14:10 light:dark cycle and all zebrafish experiments and husbandry followed standard protocols. AB, TL and ABxTup wild-type strains were used in this study. *prp1* (ua5003/ua5003), *prp2* (ua5001/5001), *prp3 (*u509/u509*), adrb2a (*u511/u511) and *pgrmc1 (*u512/u512*)* mutants were outcrossed multiple times and *prp3* F5 generation, *pgrmc1* F2 and *adrb2a* F2 generations were used for behaviour. Ethical approval for zebrafish experiments was obtained from the Home Office UK under the Animal Scientific Procedures Act 1986 with Project licence numbers 70/7612 and PA8D4D0E5.

Aβ preparations

HFIP treated Aβ42 peptide (JPT Peptide Technologies), Aβ42-1 reversed peptide (Sigma), or Aβ42 arctic peptide (Sigma), were dissolved in DMSO, vortexed occasionally for 12 min at room temperature and sonicated for 5 min to obtain 100 μM solution. The stock solutions were aliquoted as 5 μl in individual tubes and are kept are -80ºC. 1 μl of the 100 μM stock was diluted in (Phosphate buffered saline) PBS to yield 10 μM solutions which were incubated at 4°C, 25°C or 37°C for 24 hours (1 hour for arctic). 1 hour before injecting, this stock was diluted to 10 nM using 1:10 serial dilutions in PBS and kept at the respective temperature (4ºC, 25ºC, 37ºC) until injecting.

Transmission Electron Microscopy (TEM)

1 µl of (4ºC, 25ºC or 37ºC incubated) 10 µM Aβ solution was loaded onto formvar/carbon coated 300 mesh grids from Agar Scientific. The grid was washed twice in 20 mM phosphate buffer for 10 seconds and negatively stained in 2% aqueous uranyl acetate for 30 seconds. After drying for 2-3 days, samples were imaged using a Phillips TEM. At least 5 micrographs were used for each condition to blindly measure the length of the Aβ42 oligomeric structures using at least 30 measurements/condition. Using FIJI, 30-50 measurements were taken for each condition by drawing a free-hand line on the fibril, which was then scaled using the scale bar.

Heart injections

Injections were carried out blindly with a Pneumatic PicoPump (WPI) and glass capillary needles (Science Products Gmbh) prepared with a Micropipette Puller (Shutter Instruments). 5 dpf larvae were anesthetized using 4%Tricaine (42 mg/L MS222 (Sigma)) 30 min before injections. Larvae were immobilized in 1.8 % low melting point agarose (ThermoFischer) in fish water on their sides on a slide. Aβ was injected at 10 nM-1ul concentration, 1 nl into the heart chamber of the fish along with a high molecular weight fluorescent dye (2000 kDa dextran-conjugated FITC (3 mg/ml, Sigma). We estimated that 1 nl of a 10 nM Aβ injection into a ~3.01 (±0.16) x10^8 µm^3 (285-317 nL) 5dpf larva[43] yields a final monomeric brain/CSF concentration of ~28-32 pM. The success of the injection was checked under a standard fluorescent scope by the presence of fluorescence in the heart of the animal. Larvae were transferred to fresh fish water for 20 min to recover from Tricaine and transferred to sleep/wake behaviour box. For drug blocking experiments, zebrafish were soaked into 3 nM Chicago Sky Blue 6B (Sigma), 5 µM MPEP (Cambridge Biosciences), 300 nM Saracatinib (Generon) 1 day before the injections.

Fluorescently tagged HiLyte™ Fluor 647-labeled Aβ42 (Eurogentech LTD) was injected at 10 µM.

Behavioural experiments

Larval zebrafish behavioural experiments were performed and analysed as described[19]. Briefly, 5 dpf larvae were transferred to 96 square-well plates and continuously illuminated with IR and white lights from 9 am to 11 pm in a Zebrabox (Viewpoint life sciences) for 24-48 hours. The movement of each larva was measured and duration of movement was recorded with an integration time of 10 sec. Data were processed using custom PERL and MATLAB (The Mathworks, R2015a) scripts, and statistical tests were performed using MATLAB. Mutant larval zebrafish experiments were performed on siblings from heterozygous in-crosses, differing only in the mutation of the specific gene and genotyped at the end of the experiment.

In situ hybridization

RNA in situ hybridization to detect *c-fos* was performed as described before (Thisse &Thisse, 2007). Zebrafish larvae were fixed in 4% paraformaldehyde in PBS at 4°C overnight. A template for in vitro transcription was generated by PCR using a reverse primer that contains a T7 promoter sequence 5'-TAATACGACTCACTATAGGG-3' from cDNA. A digoxygenin (DIG)-labelled antisense RNA probe was synthesized using the DIG labelling kit (Roche) and T7 RNA polymerase according to the manufacturer's recommendations. The probe was detected with anti-DIG-AP antibody (1:2,000, Roche) and nitro-blue tetrazolium chloride (NBT)/5-bromo-4-chloro-3′-indolyphosphate (BCIP) substrate (Roche) according to published protocols. Embryos were stored in 60% glycerol/PBS for imaging.

KASP genotyping

For rapid genotyping of mutant zebrafish harbouring the *prp3Δ8*, *adrb2aΔ8* and *pgrmc1Δ16* alleles, a mutant allele-specific forward primer, a wild-type allele-specific forward primer and a common reverse primer were used (LGC Genomics). The primer sequences were targeted against the following;

prp3

5'TTTTCGCAGCTCCTGTGGGGATGCWTTCCAAATTTAAGCTCTTCTCCTTCCTAAACTG
CCTGTTGCTGCTGGCTGTGCTGCTACCGGTAGCGCAGTCT**[CGCCGGGG/-]**CGG
GGGCTTCGGACGTGGCGGCGGGAGAGGTGGAGGCTGGGGAGGCAGCAGCTCGGGTC
GCGCGGGCTGGGGTGCAGCTGGAGGGCATCACCGAGCTCCACCCGTACACACGGGACAC-3'

adrb2a

5'TTTTACTACTTACTGTTTGCACAAACCTATGTTAACTGTGTTAACGTGTTTTCTTCT
GCTTTTCTTTCTTGATCTCTGTCAGGTCATGGGAAACATAAGGTCCTCAATACC**[CGA**
AGATC/-]TTATCTGTCCAAACAATACTAATGCCTCCACCAAAAGCGAACTACAGATG
ACAGTGCTGGGCACACTCATGTCCATTCTTGTCTTGATCATCGTCTTTGGCAATGTGA
TGGTGATTACAGCCA-3'

pgrmc1:

5’ATGGCTGAAGAAGCAGTCGAGCAAACTTCTGGAATCCTTCAGGAAATTTTCACGT
CGCCACTGAACATCAGTTTGCTATGTCTTTGTTTGTTCCTACTTTACAAAATCATCCG
CGGAGACAAGCC**[TGCAGACTATGGCCCG/-]**GYTGAGGAGCCGCTGCCCAAACT
CAAGAAAAGAGATTTYACTTTAGCAGATCTGCAAGAGTACGATGGACTGAAAAACC
CAAGAATCCTGATGGCTGTCAACGGG-3’

where [x/-] indicates the indel difference in [WT/mutant]. PCR amplification was performed using KASP Master mix (LGC Genomics) according to the manufacturer’s instructions. Fluorescence was read on a CFX96 Touch Real-Time PCR Detection System (Bio-Rad) and the allelic discrimination plot generated using Bio-Rad CFX Manager Software.

Time lapse confocal microscopy

Three Casper fish at 5 dpf were mounted dorsally on a slide in 1.5% agarose. 10 nl of Aβ42-Hi488 was intra-cardiac injected to embryos, control fish were untreated. Fish were imaged for 6 min taking 2 μm thick stacks through the whole brain using a confocal microscope (Leica SP8). Each fish was imaged every 20 mins for 8 hours.

pERK/tERK staining and activity Mapping

Larvae were fixed overnight at 4°C in 4% paraformaldehyde (PFA) and 4% sucrose in PBS; permeabilized 45 min in 0.05% trypsin-EDTA on ice; blocked 6 hr at room temperature (RT) in phosphate buffered saline plus 0.05% Triton (PBT) plus 2% normal goat serum, 1% BSA, and 1% DMSO; and then incubated over sequential nights at 4°C in primary antibodies (Cell Signaling Technology 4370 and 4696; 1:500) and secondary antibodies conjugated with Alexa

fluorophores (Life Technologies; 1:200) in PBT plus 1% BSA and 1% DMSO.

Larvae were mounted in 1.5% low melt agarose and imaged with a custom two-photon microscope (Bruker; Prairie View software) with a 203 water immersion objective (Olympus). Images were noise filtered using a custom MATLAB (The MathWorks) scripts and registered into Z-Brain using the Computational Morphometry Toolkit (http://www.nitrc.org/projects/cmtk/) with the command string: -a -w -r 0102 -l af -X 52 -C 8 -G 80 -R 3 -A "–accuracy 0.4 –auto-multi-levels 4" -W "–accuracy 1.6" -T 4. Registered images were prepared using a custom MATLAB/MIJ (http://bigwww.epfl.ch/sage/soft/mij/) script to downsize, blur, and adjust the maximum brightness of each stack to the top 0.1% of pixel intensities to preserve dynamic range. Activity maps were generated using MATLAB scripts[22].

Crispr/Cas9 mutant generation

The CRISPR design tool CHOPCHOP (http://chopchop.cbu.uib.no) was used to identify a target region in zebrafish *prp3*, *adrb2a* and *pgrmc1*. The gene specific oligomers were ordered from Thermofisher including the 5’ and 3’ tags:

for *prp3:*

5’ATTTAGGTGACACTATA<u>GTAGCGCAGTCTCGCCGGGG</u>GTTTTAGAGCTAGAAATAGCAAG-3’

For *adrb2a*:

5’ATTTAGGTGACACTATA<u>GTTTGGACAGATAAGATCTT</u>GTTTTAGAGCTAGAAATAGCAAG-3’

For *pgrmc1*:

5'ATTTAGGTGACACTATATGCAGACTATGGCCCGGTTGGTTTTAGAGCTAGAAATAG CAAG-3'

Constant oligomer:

5'AAAAGCACCGACTCGGTGCCACTTTTTCAAGTTGATAACGGACTAGCCTTATTTTA ACTTGCTATTTCT AGCTCTAAAAC-3'

The constant oligomer and the gene specific oligomer were annealed on a PCR machine and filled in using T4 DNA polymerase (NEB)[44]. The template was cleaned up using a PCR clean-up column (Qiaquick) and the product was verified on a 2% agarose gel. The sgRNA was transcribed from this DNA template using Ambion MEGAscript SP6 kit[44]. Cas9 mRNA and the purified sgRNA were co-injected into one-cell stage embryos at a concentration of 200 ng and 100 ng per embryo, respectively.

Caspase-3 staining

5dpf larvae that were injected with Aβ oligomers or soaked in Camptothecin (1μM; Sigma Aldrich) were fixed 5 hours after injection/drug treatment in 4% PFA and kept overnight at 4℃. Brains were dissected and dehydrated next day and were washed 3 times in PDT buffer (0.3 Triton-X in PBST with 1% DMSO) and incubated with Caspase-3 antibody (1:500; BD Biosciences) at 4℃. The brains were incubated with Alexa Fluor 568 goat anti-rabbit antibody (1:200; Invitrogen) next day at 4℃ overnight and imaged using a confocal microscope.

Statistical Analyses

Details of statistics used in each panel are also described in the figure legend. For multiple comparisons, data was first tested for normality by the Kogloromov-Smirnov (KS) statistic and

extreme outliers were discarded by Grubb's test ($p \leq 0.05$). Those that violated normality were analysed with the non-parametric Kruskal-Wallis test, with either Tukey-Kramer or Bonferonni post hoc testing; otherwise, data was analysed with one-way ANOVA followed by Tukey's post-hoc testing. For dose response curves, a two-way ANOVA was performed to test the interaction effects between preparation type and dose. For return to baseline statistics, paired t-tests were performed. Survival curves were analysed with Kaplan-Meier log rank test. All statistical tests and graphs were generated in MATLAB (R2015a) loaded with the Statistical Toolbox. Injection and tracking experiments were performed blinded.

Supplementary Figure Legends

Fig. S1. Aβ oligomers exert dose-dependent, short-term effects on zebrafish sleep

A) Same images from Fig. 1B, highlighting the region of interest in the telencephalon for fluorescence intensity measurements in B. Anterior is to the top, dorsal view.

B) Heart-injected fluorescently-tagged Aβ (black) penetrates the brain within 1 hr and peaks in concentration 2-3 hr post-injection. Cyan shows background fluorescence of a negative control. The shaded area shows ± standard deviation from 3 independent injections.

C) Electron micrographs of Aβ oligomers formed after 24 hr incubation at 4ºC (A), 25ºC (B), 37ºC (C), and $A\beta^{arctic}$ (as control) incubated at 25ºC for 2 hr (D). The color code is used throughout the main and supplementary figures. Scale bar = 100 nm

D) The $A\beta^{short}$ (blue) and $A\beta^{long}$ (green) have opposing, dose-dependent effects on average waking activity. $p \leq 0.001$, prep effect; doseXprep interaction $p \leq 0.01$, two-way ANOVA. Each dot represents a single larval injection. The error bars represent ± the SEM.

E) $A\beta^{short}$ (blue) and $A\beta^{long}$ (green) have opposing, dose-dependent effects on sleep. $p \leq 0.05$, prep effect; doseXprep interaction $p=0.08$, two-way ANOVA. Based on the data in D-E, 10nM was chosen as the concentration for all subsequent Aβ injection experiments.

F-I) The effects of $A\beta^{short}$ (F,G) and $A\beta^{long}$ (H,I) on waking activity (top) and sleep (bottom) return to baseline after 24hr. Shown in F and H are traces for 48 hours post-injection on a 14hr:10hr light:dark cycle (indicated by the white and black bars). The ribbons represent ± the SEM. Plotted in G and I are the percent change induced by Aβ relative to $A\beta^{rev}$ for day 1 versus day 2, demonstrating that these parameters return to baseline (*$p \leq 0.01$, paired t-test). Each line represents a single larva, the thicker line represents the mean ± SEM.

J-K) Aβ oligomers have no significant effects on waking activity or sleep during the first post-injection night (same injections as in Fig. 1G-J). Each dot represents a single larva, normalized to the $A\beta^{rev}$ control injections. The data is combined from n=4 independent experiments.

Fig. S2. Aβ exposure does not increase neuronal cell death and does not alter survival into adulthood.

A) Dorsal and ventral views of representative 5 dpf larval brains stained for Caspase-3 activation (purple) to map apoptosis. Exposure to the topoisomerase inhibitor camptothecin (CPT, 1µM), which induces apoptosis, serves as a positive control. DAPI stains nuclei in white for reference. Anterior is to the left.

B,C) Quantification of the number of Caspase-3 positive cells after exposure to 1µM CPT or Aβ oligomer injections (n=5 brains for each condition, B-dorsal, C-ventral). Only CPT significantly increased apoptosis relative to $A\beta^{rev}$. ns, $p>0.05$, one-way ANOVA, Tukey's post-hoc test.

D) Survival curves to adulthood after 5dpf injection of Aβ oligomers. There are no significant differences among survival curves, $p>0.05$, Kaplan-Meier log rank test.

<u>Fig. S3</u>. Crispr/Cas9 targeting of zebrafish *adrb2a* and *pgrmc1*

A) Human and zebrafish PGRMC1 contain a conserved Transmembrane (TM) domain (yellow) and a Cytochrome b5-like Heme/Steroid binding domain (blue).

B) Protein alignment of zebrafish Pgrmc1 to human PGRMC1. Identical residues are marked in black, similar residues in grey.

C) Crispr-Cas9 targeting of *pgrmc1* generated an allele with a 16bp deletion. The PAM sequence is indicated in red.

D) The predicted translation of *pgrmc1* Δ16 leads to a premature stop codon.

E) Protein alignment of zebrafish Adrb2a and Adrb2b to human ADRB2. Identical residues are marked in black, similar residues in grey. The N-terminal region (pink) is the putative Aβ binding region. The C-terminal region is in green.

F) Crispr-Cas9 targeting of *adrb2a* generated an allele with an 8bp deletion. The PAM sequence is indicated in red.

G) The predicted translation of *adrb2a*Δ8 leads to a premature stop codon lacking all functional domains.

<u>Fig. S4</u>. *adrb2a* and *pgrmc1* mutations have small effects on baseline sleep:wake parameters.

A-C') Sleep and waking activity plots for larvae from *pgrmc1*$^{+/-}$ in-crosses. A,A') show representative 48hr traces for the indicated genotypes. The ribbon represents ± SEM. B-C') Sleep and waking activity for each larva for all genotypes are plotted. The error bars represent

the mean ± SEM. There is a trend to decreased waking activity in *pgrmc1*$^{-/-}$ mutants compared to wild type siblings. p=0.07, Kruskal-Wallis, Tukey-Kramer post-hoc.

D-F') Sleep and waking activity plots for larvae from *adrb2a*$^{+/-}$ in-crosses. D,D') show 48 hr traces for all three genotypes. The ribbon represents ± SEM. E-F') Sleep and waking activity for the day and night are plotted for each larva. The error bars represent the mean ± SEM. Compared to both wild type and heterozygous siblings, *adrb2a*$^{-/-}$ mutants have increased sleep during the day. *p≤0.05, Kruskal-Wallis, Tukey-Kramer post-hoc.

Fig. S5. Relationship among zebrafish *prp* genes and Crispr-Cas9 targeting of *prp3*.

A) Schematic comparing zebrafish Prp1-3 proteins to human Prp. SP, signal peptide (dark grey); R, repetitive region (blue); HD, hydrophobic domain (yellow); N, glycosylation sites (black lines); GPI anchor residue (triangle); hydrophobic tail (coral). Aβ oligomer binding regions are shown in red. Breakpoints at repetitive regions indicate length variation. Adapted from [45].

B) Protein alignments of zebrafish Prp1, Prp2, and Prp3 proteins to human and mouse Prp proteins. Identical residues are marked in black, similar residues in grey. Aβ oligomer binding sites are indicated in red. The site of truncation mutations in *prp1* and *prp2* mutants are indicated with a triangle.

C) Crispr-Cas9 targeting of *prp3* generated an allele with an 8bp deletion. The PAM sequence is indicated in red.

D) The *prp3*$^{\Delta 8}$ allele is predicted to encode a frameshifted protein after amino acid 27 and a premature stop codon. The Prp3$^{\Delta 8}$ protein lacks all the functional domains shown in A.

<u>Fig. S6</u>. *prp* double and triple mutants do not affect baseline sleep or wake across the day:night cycle.

A-C') Sleep and waking activity plots for larvae from *prp1*$^{+/-}$; *prp2*$^{+/-}$ in-crosses. A,A') show representative 48hr traces for the indicated genotypes. The ribbon represents ± SEM. B-C') Sleep and waking activity for each larva for all genotypes are plotted. The error bars represent the mean ± SEM.

D-F') Sleep and waking activity plots for larvae from *prp1*$^{+/-}$;*prp2*$^{-/-}$ in-crosses. D,D') show 48 hr traces for all three genotypes. The ribbon represents ± SEM. E-F') Sleep and waking activity for the day and night are plotted for each larva. The error bars represent the mean ± SEM.

G-I') Prp3 does not modify the *prp1*$^{-/-}$;*prp2*$^{-/-}$ mutant sleep and wake phenotypes, as shown in sleep and waking activity plots for larvae from *prp1*$^{-/-}$;*prp2*$^{-/-}$;*prp3*$^{+/-}$ in-crosses. G,G') show 48 hr traces for all three genotypes. The ribbon represents ± SEM. H-I') Sleep and waking activity for the day and night are plotted for each larva. The error bars represent the mean ± SEM.

<u>Fig. S7</u>. The response to Aβ oligomers by *prp1*$^{-/-}$;*prp2*$^{-/-}$ mutants is only partially modulated by *prp3*.

A-B) The effect of Aβ^{short} and Aβ^{long} on the waking activity of 5 dpf larvae, normalized to the Aβ reverse control, in wild type and *prp* mutants during the day post injection. The enhancement of waking activity by Aβ^{short} is similarly enhanced in *prp1*$^{-/-}$;*prp2*$^{-/-}$ double and *prp1*$^{-/-}$;*prp2*$^{-/-}$;*prp3*$^{-/-}$ mutants (A), while the suppression of activity by Aβ^{long} is blocked in both *prp1,2* double and *prp1,2,3* triple mutants (B). $^{ns}p>0.05$; $^{*}p\leq0.05$, Kruskal-Wallis, Tukey-Kramer post hoc test. The error bars represent the mean ± SEM.

C-D) The effect of $A\beta^{short}$ and $A\beta^{long}$ on post-injection sleep of 5 dpf wild type and *prp* mutant larvae, normalized to the $A\beta^{rev}$ controls. The reduction in sleep induced by $A\beta^{short}$ is stronger in *prp1*$^{-/-}$;*prp2*$^{-/-}$;*prp3*$^{-/-}$ triple mutants compared to in *prp1*$^{-/-}$;*prp2*$^{-/-}$ double mutants (C), while the induction of sleep by $A\beta^{long}$ is blocked in both *prp1,2* double and *prp1,2,3* triple mutants (D). $^{ns}p>0.05$; $^{*}p\leq0.05$, $^{**}p\leq0.001$, Kruskal-Wallis, Tukey-Kramer post hoc test. The error bars represent the mean ± SEM.

E) Representative traces of waking activity after $A\beta^{long}$ versus $A\beta^{reverse}$ injections in wild type larvae in the absence (top) or presence (bottom) of the Aβ-Prion disruptor, Chicago Sky Blue (3nM). The data are from the same injections as in Figure 4F. Ribbons represent ± SEM. Light and dark bars indicate the lights ON and lights OFF periods, respectively.

F) The percent change in waking activity induced by $A\beta^{long}$ relative to $A\beta^{rev}$ control injections in the absence or presence of 3nM Chicago Sky Blue. $^{**}p\leq0.01$, Kruskal-Wallis. Each dot represents a single larva and error bars indicate ± SEM.

G) Representative traces of sleep behaviour after $A\beta^{long}$ versus $A\beta^{rev}$ injections in the absence or presence of the Src-kinase inhibitor, saracatinib (300nM) or mGluR5 inhibitor, MPEP (5 µM). Ribbons represent ± SEM. The data are from the same injections as in Fig. 4H-J.

H) The percent change in sleep induced by $A\beta^{long}$ relative to $A\beta^{rev}$ control injections in the absence or presence of MPEP (5 µM) and (300nM) saracatinib. $^{ns}p>0.05$,$^{*}p\leq0.05$ Kruskal-Wallis, Tukey-Kramer post-hoc. Each dot represents a single larva and error bars indicate ± SEM. Data is pooled from 2 independent experiments.

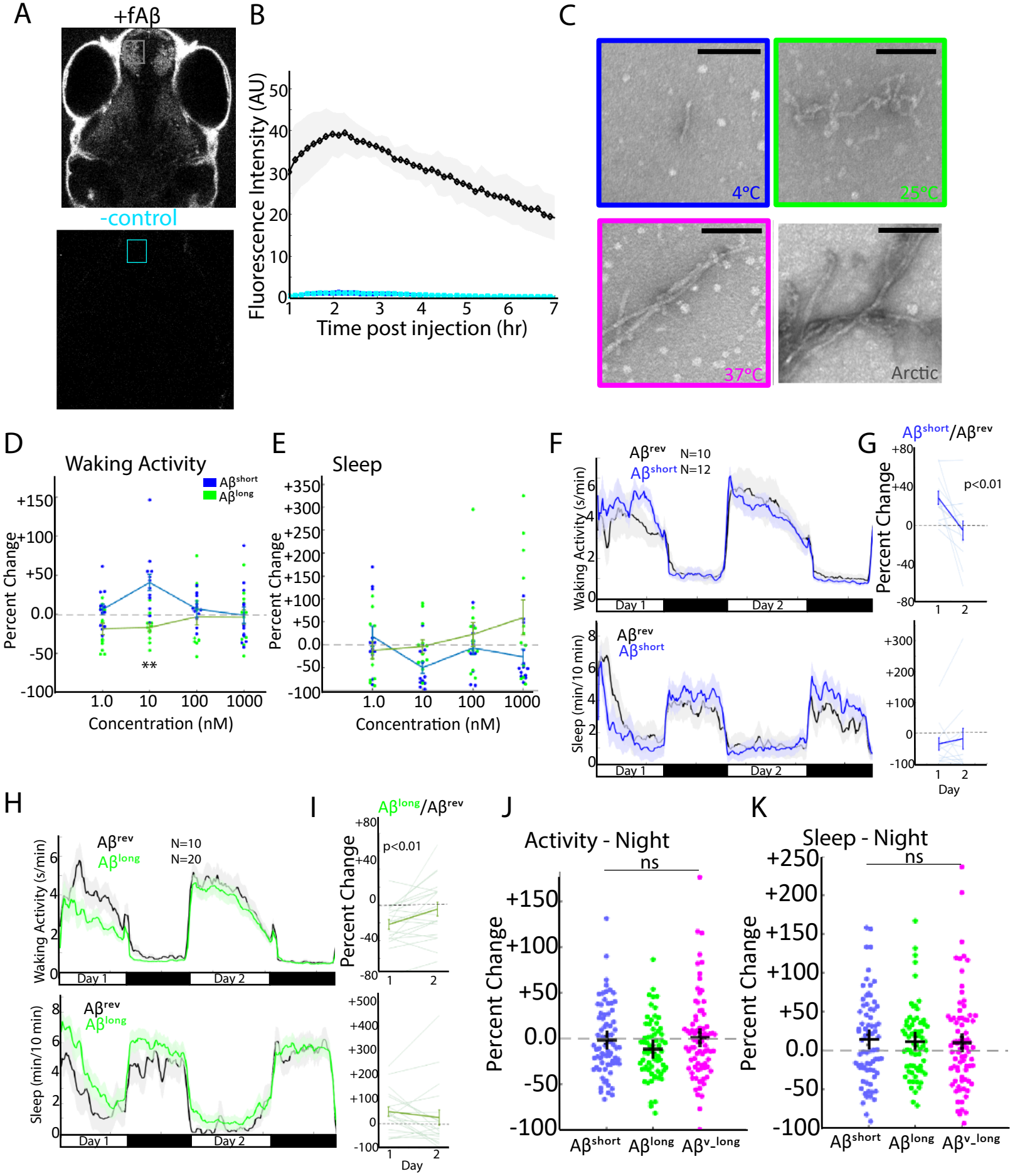
A
+fAβ
-control
B
Fluorescence Intensity (AU)
Time post injection (hr)
C
4°C
25°C
37°C
Arctic
D
Waking Activity
Percent Change
Concentration (nM)
E
Sleep
F
Waking Activity (s/min)
Sleep (min/10 min)
Day 1
Day 2
G
Percent Change
p<0.01
Day
H
I
p<0.01
J
Activity - Night
ns
K
Sleep - Night
ns

Figure S1

A.

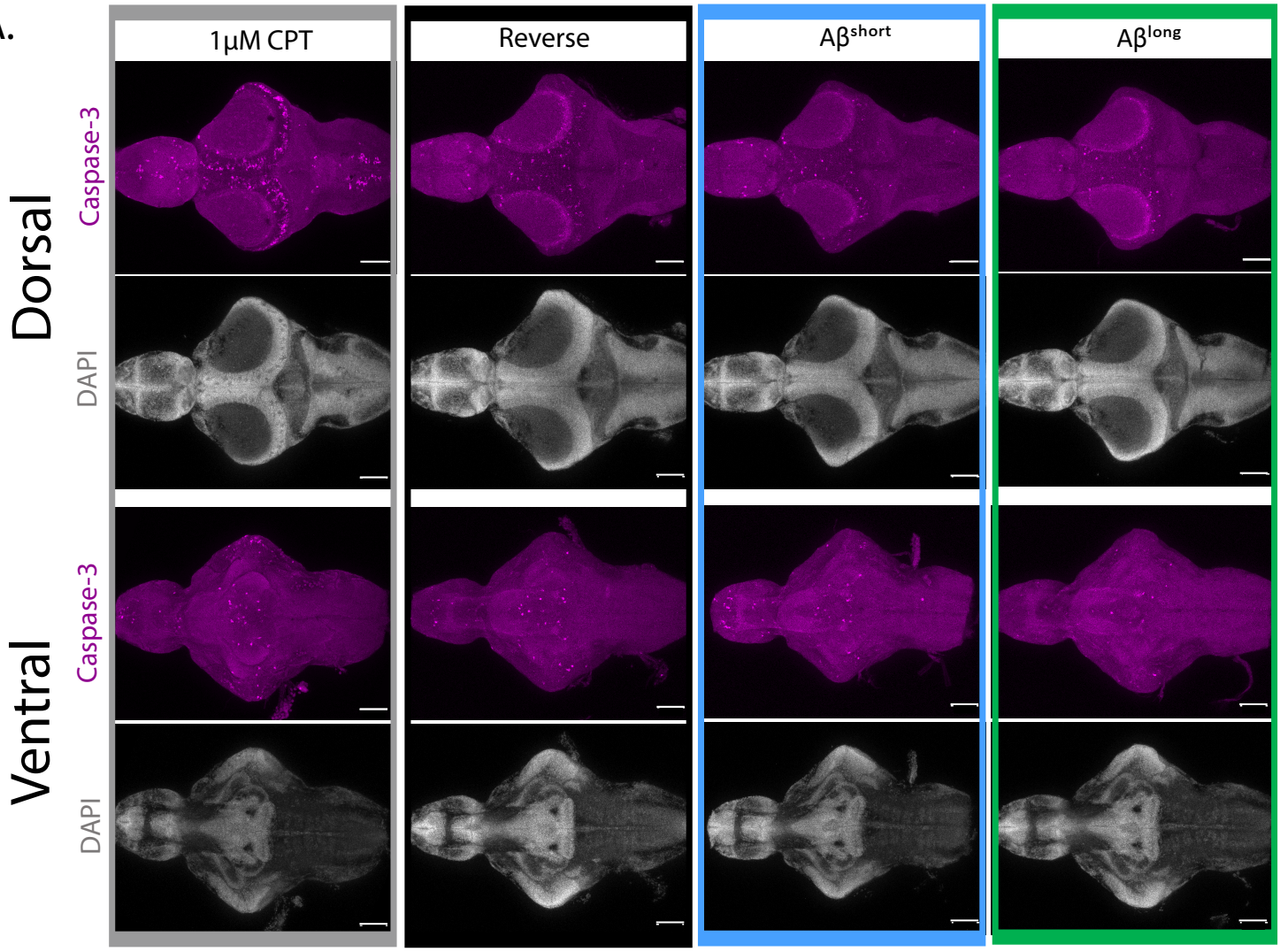

B.

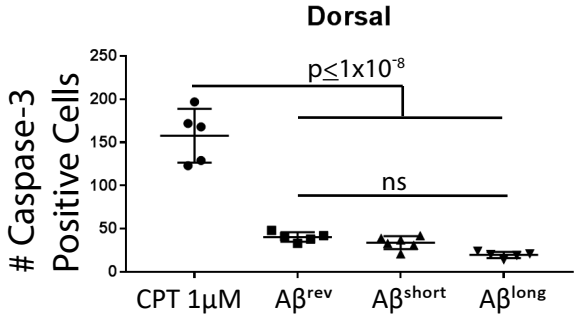

C.

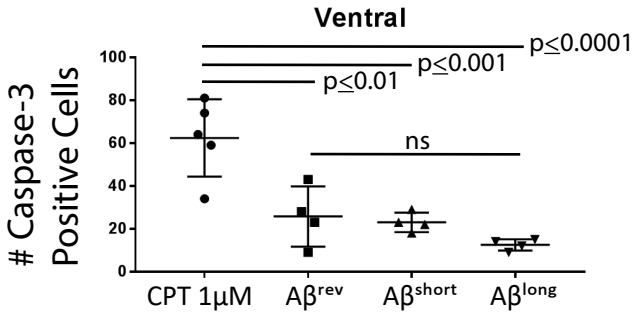

D.

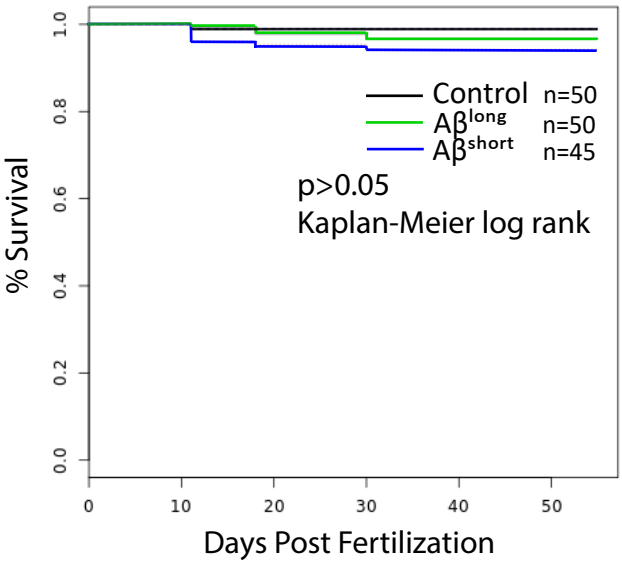

Figure S2

A

B

```
zPGRMC1     1 MAEEAVEQT---------SGILQEIFTSPLNISLLCLCLFLLYKIIRGDKPADYGPVE--
hPGRMC1     1 MAAEDVVATGADPSDLESGGLLHEIFTSPLNLLLLGLCIFLLYKIVRGDQPAASGDSDDD

zPGRMC1    50 --EPLPKLKKRDFTLADLQEYDGLKNPRILMAVNGKVFDVTRGKKFYGPEGPYGVFAGKD
hPGRMC1    61 EPPPLPRLKRRDFTPAELRRFDGVQDPRILMAINGKVFDVTKGRKFYGPEGPYGVFAGRD

zPGRMC1   108 ASRGLATFCLEKEALKDTHDDLSDLNAMQQESLSEWETQFTQKYDYIGKLLKPGEEPTEY
hPGRMC1   121 ASRGLATFCLDKEALKDEYDDLSDLTAAQQETLSDWESQFTFKYHHVGKLLKEGEEPTVY

zPGRMC1   168 TDDEEVKDK---KKD
hPGRMC1   181 SDEEEPKDESARKND
```

C

```
                121
pgrmc1 WT    5'…CCGCGGAGACAAGCCTGCAGACTATGGCCCGGTTGAGGAGCCGCTGCCC
pgrmc1Δ16    5'…CCGCGGAGACAAGCC –GC - - - - - - - - - - - - - - - - TGAGGAGCCGCTGCCC
```

D

```
                31                  43                                  179
PGRMC1 WT    …FLLYKIIRGDKP ADYGPVEE PLPKLKKRDFTLAD……Stop
PGRMC1 Δ16   …FLLYKIIRGDKP LRSRCPNSRKEILLStop
                                43                  57
```

E

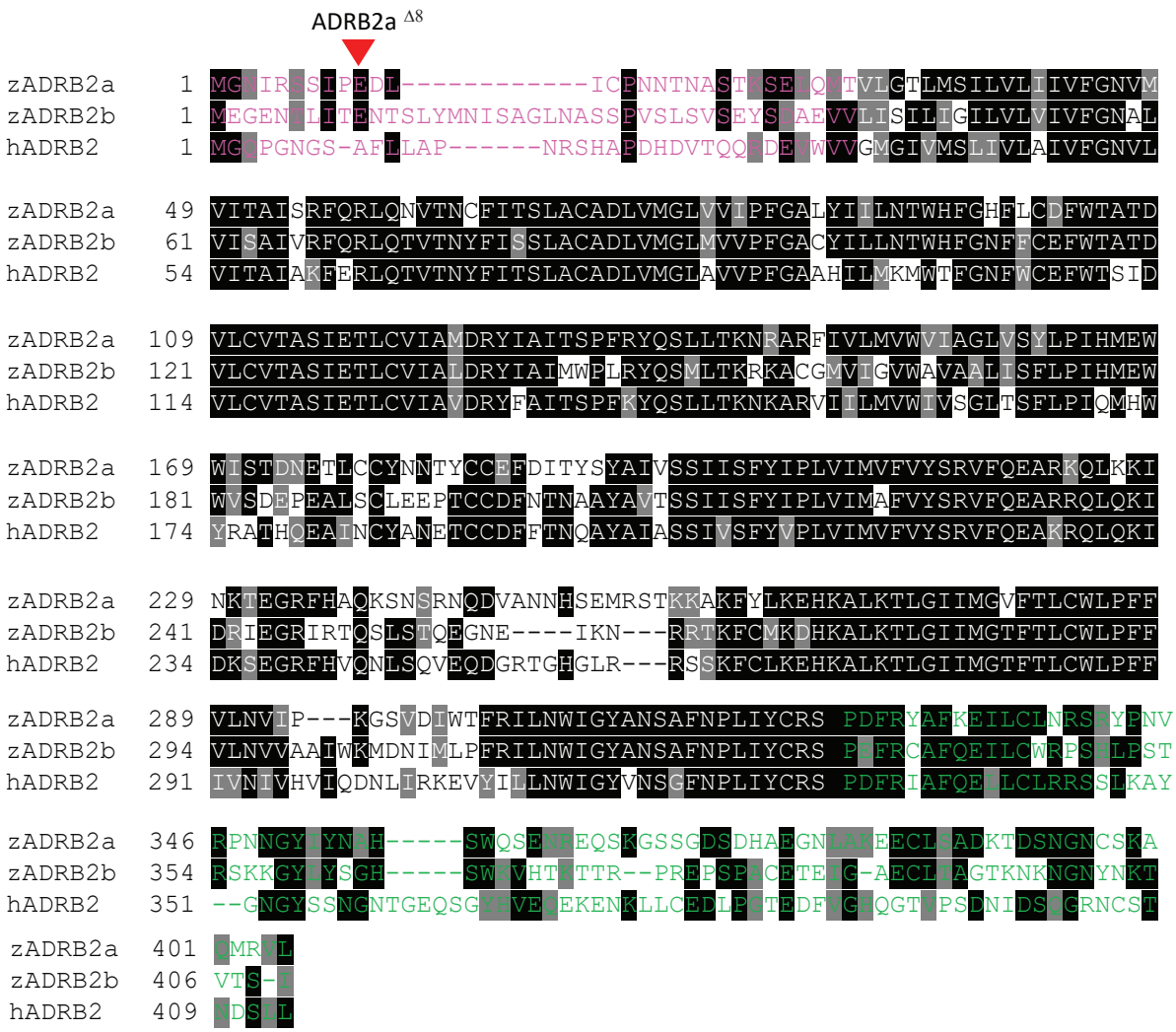

F

```
                1
adrb2a WT       ATGGGAAACATAAGGTCCTCAATACCCGAAGATCTTATCTGTCCAAACAATACTAATG
adrb2a   Δ8     ATGGGAAACATAAGGTCCTCAATACC - - - - - - - -TTATCTGTCCAAACAATACTAATG
```

G

```
                1                                                    405
ADRB2a WT       MGNIRSSIP EDLICPNNTNAST…….. …….. Stop
ADRB2a Δ8       MGNIRSSIP YLSKQYStop
                1                16
```

Figure S3

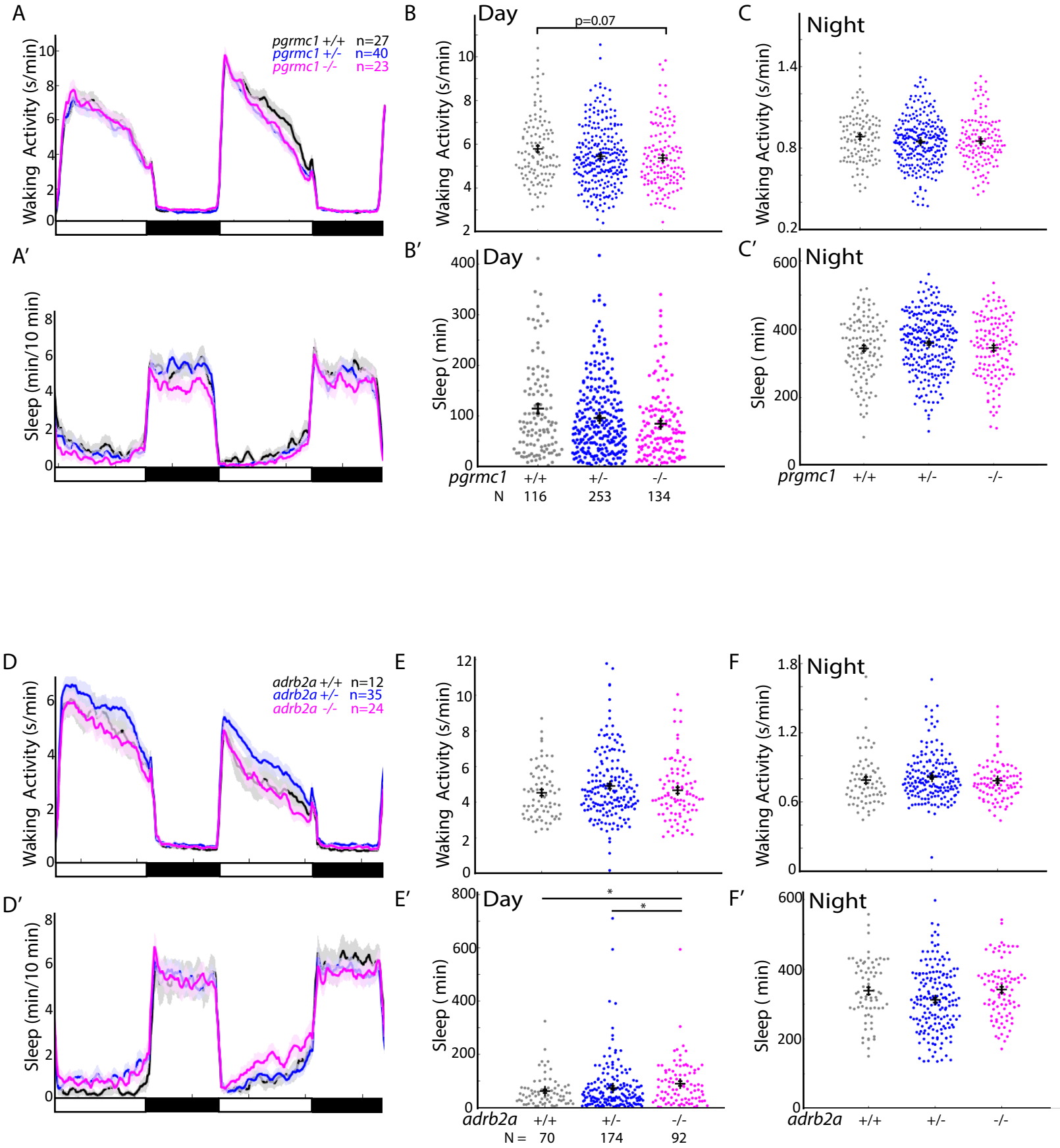
A
pgrmc1 +/+ n=27
pgrmc1 +/- n=40
pgrmc1 -/- n=23
Waking Activity (s/min)
B
Day
p=0.07
Waking Activity (s/min)
C
Night
Waking Activity (s/min)
A'
Sleep (min/10 min)
B'
Day
Sleep (min)
pgrmc1 +/+ +/- -/-
N 116 253 134
C'
Night
Sleep (min)
prgmc1 +/+ +/- -/-
D
adrb2a +/+ n=12
adrb2a +/- n=35
adrb2a -/- n=24
Waking Activity (s/min)
E
Waking Activity (s/min)
F
Night
Waking Activity (s/min)
D'
Sleep (min/10 min)
E'
Day
Sleep (min)
adrb2a +/+ +/- -/-
N = 70 174 92
F'
Night
Sleep (min)
adrb2a +/+ +/- -/-

Figure S4

A

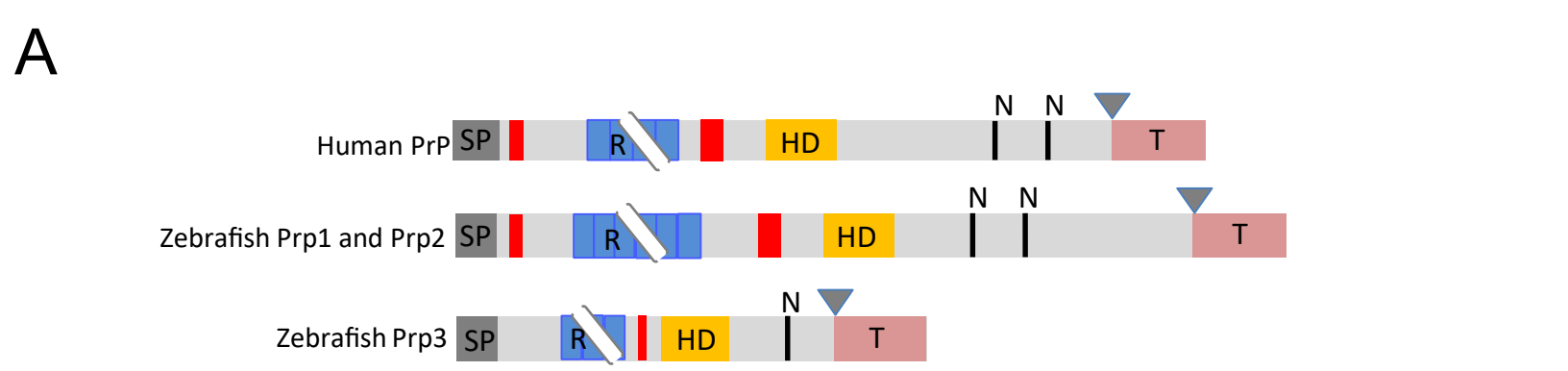

B

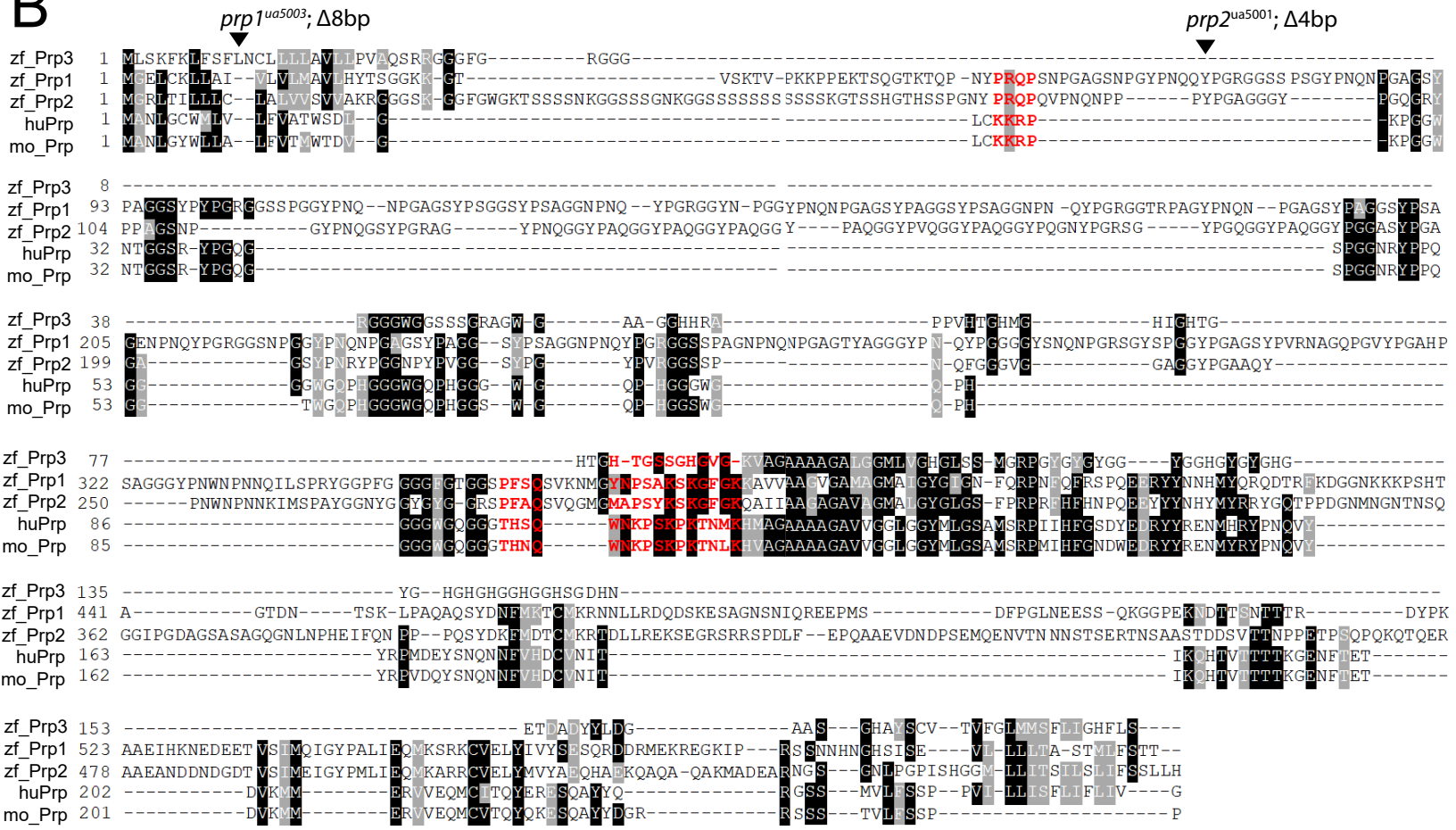

C

Prp3 WT 5' ***GTAGCGCAGTCTCGCCGGGG*****CGG**GGGCTTCGGACGTGGCGGCGGGAGA

Prp3 △8 5' ***GTAGCGCAGTCT*** - - - - - - - - **CGG**GGGCTTCGGACGTGGCGGCGGGAGA

D

1 27 188

WT: MLSKFKLFSFLNCLLLLAVLLPVAQSR RGGGFGRGGGR.....STOP

Prp3 △8 : MLSKFKLFSFLNCLLLLAVLLPVAQSR GLRTWRRERWR.....STOP

1 27 148

Figure S5

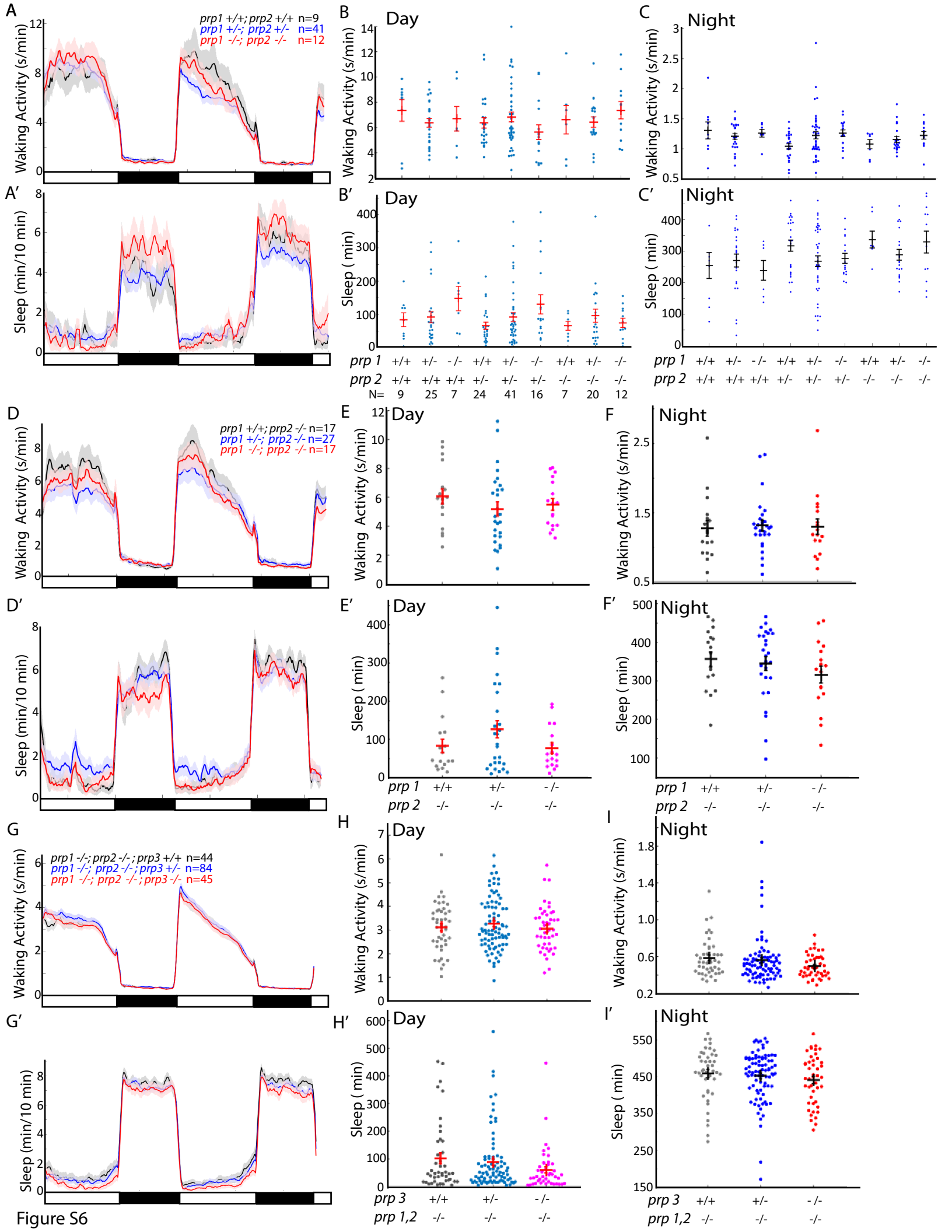
A
prp1 +/+; prp2 +/+ n=9
prp1 +/-; prp2 +/- n=41
prp1 -/-; prp2 -/- n=12
Waking Activity (s/min)
B
Day
C
Night
A'
Sleep (min/10 min)
B'
Sleep (min)
C'
prp 1 +/+ +/- -/- +/+ +/- -/- +/+ +/- -/-
prp 2 +/+ +/+ +/+ +/- +/- +/- -/- -/- -/-
N= 9 25 7 24 41 16 7 20 12
D
prp1 +/+; prp2 -/- n=17
prp1 +/-; prp2 -/- n=27
prp1 -/-; prp2 -/- n=17
E
F
D'
E'
F'
prp 1 +/+ +/- -/-
prp 2 -/- -/- -/-
G
prp1 -/-; prp2 -/- ; prp3 +/+ n=44
prp1 -/-; prp2 -/- ; prp3 +/- n=84
prp1 -/-; prp2 -/- ; prp3 -/- n=45
H
I
G'
H'
I'
prp 3 +/+ +/- -/-
prp 1,2 -/- -/- -/-

Figure S6

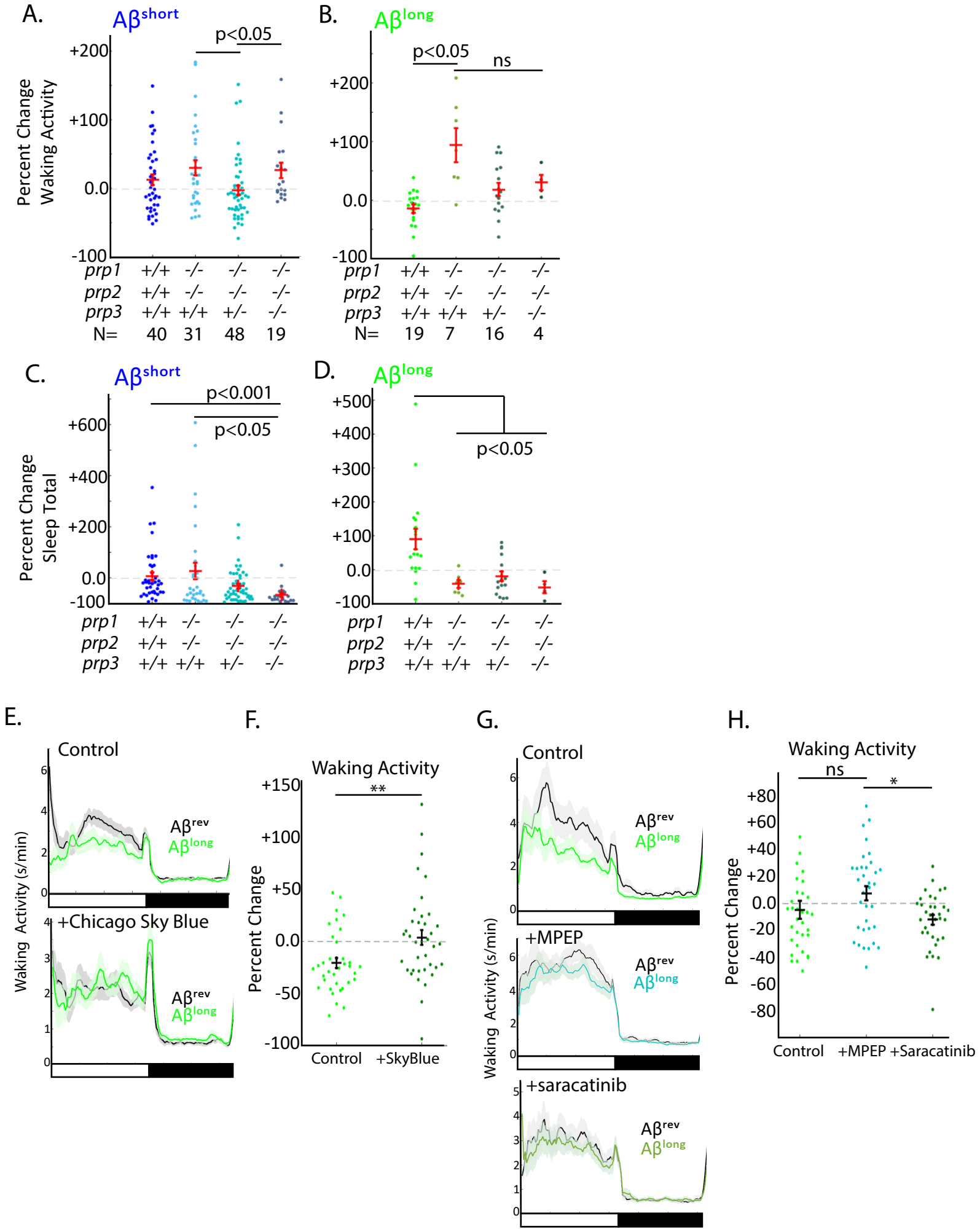
A.
Aβshort
p<0.05
Percent Change Waking Activity
+200
+100
0.0
-100
prp1 +/+ -/- -/- -/-
prp2 +/+ -/- -/- -/-
prp3 +/+ +/+ +/- -/-
N= 40 31 48 19
B.
Aβlong
p<0.05
ns
+200
+100
0.0
-100
prp1 +/+ -/- -/- -/-
prp2 +/+ -/- -/- -/-
prp3 +/+ +/+ +/- -/-
N= 19 7 16 4
C.
Aβshort
p<0.001
p<0.05
Percent Change Sleep Total
+600
+400
+200
0.0
-100
prp1 +/+ -/- -/- -/-
prp2 +/+ -/- -/- -/-
prp3 +/+ +/+ +/- -/-
D.
Aβlong
p<0.05
+500
+400
+300
+200
+100
0.0
-100
prp1 +/+ -/- -/- -/-
prp2 +/+ -/- -/- -/-
prp3 +/+ +/+ +/- -/-
E.
Control
Aβrev
Aβlong
Waking Activity (s/min)
+Chicago Sky Blue
Aβrev
Aβlong
F.
Waking Activity
**
Percent Change
+150
+100
+50
0.0
-50
-100
Control
+SkyBlue
G.
Control
Aβrev
Aβlong
Waking Activity (s/min)
+MPEP
Aβrev
Aβlong
+saracatinib
Aβrev
Aβlong
H.
Waking Activity
ns
*
Percent Change
+80
+60
+40
+20
0.0
-20
-40
-60
-80
Control
+MPEP
+Saracatinib

Figure S7